Metallomics

New aspects of Fe-Cu crosstalk uncovered by transcriptomic characterization of Col-0 and the copper uptake mutant spl7 in Arabidopsis thaliana

Journal:	*Metallomics*
Manuscript ID	MT-ART-10-2018-000287.R1
Article Type:	Paper
Date Submitted by the Author:	03-Nov-2018
Complete List of Authors:	Ramamurthy, Raghuprakash Kastoori; University of Nebraska-Lincoln, Department of Agronomy and Horticulture Xiang, Qingyuan; University of Nebraska, Department of Agronomy and Horticulture; University of Florida, Horticultural Sciences Department Hsieh, En-Jung; University of Nebraska-Lincoln, Department of Agronomy and Horticulture; Institute of Plant and Microbial Biology Academia Sinica Liu, Kan; University of Nebraska-Lincoln, School of Biological Sciences Zhang, Chi; University of Nebraska-Lincoln, School of Biological Sciences Waters, Brian; University of Nebraska, Agronomy and Horticulture

New aspects of iron-copper crosstalk uncovered by transcriptomic characterization of Col-0 and the copper uptake mutant *spl7* in *Arabidopsis thaliana*

Raghuprakash Kastoori Ramamurthy[1], Qingyuan Xiang[1,2], En-Jung Hsieh[1,3], Kan Liu[4], Chi Zhang[4], and Brian M. Waters[1]

[1]Department of Agronomy and Horticulture, University of Nebraska-Lincoln, Lincoln, NE 68583-0915, USA; [2]Current Address, Horticultural Sciences Department, University of Florida, Gainesville, Florida, 32611; [3]Current Address, Institute of Plant and Microbial Biology, Academia Sinica, Taipei, Taiwan, [4]School of Biological Sciences, University of Nebraska-Lincoln, Lincoln, NE

Correspondence:

Brian Waters (bwaters2@unl.edu), Department of Agronomy and Horticulture, University of Nebraska-Lincoln, Lincoln, NE 68583-0915, USA

Tel: 402-472-0153 Fax: 402-472-7904

Running head: Transcriptomic characterization of Fe/Cu crosstalk in Arabidopsis

The number of tables: 4

The number of figures: 6

Number of supplementary tables: 4

Number of supplementary datasets: 1

Abstract

Iron (Fe) and copper (Cu) are essential micronutrients for energy metabolism and reactive oxygen species (ROS) scavenging. Some Cu-containing proteins can be substituted with Fe-containing proteins, and *vice versa*, while several Arabidopsis genes are regulated by both metals. Few details of how plants coordinate Fe-Cu crosstalk are known. Gene expression was measured in roots and rosettes of Fe, Cu, and simultaneously Fe and Cu deficient WT and a mutant of the Cu-uptake transcription factor *SPL7*. The *spl7* mutant accumulated excess Fe in normal conditions, and lower Fe supply rescued the growth phenotype and normalized Fe:Cu ratios. Most Fe regulated genes were expressed similarly in WT and *spl7*, although at higher fold-change levels in *spl7* mutants. Expression patterns indicated that both SPL7 and the FIT Fe uptake transcription factor influenced expression of many key Fe uptake genes. Most notably, the newly discovered *IMA*/*FEP* genes and the subgroup Ib *bHLH* genes, which are upstream of Fe uptake responses, were repressed in WT under Cu deficiency. Several AP2/ethylene response factor (*AP2/ERF*) genes and other redox homeostasis network genes were derepressed in *spl7* mutants. Together, we present new information about Fe-Cu crosstalk in plants that could be applied for developing abiotic stress tolerant crops.

Significance to metallomics: These results give new insights into iron-copper crosstalk mechanisms in roots and leaves of plants, and show that many metal and redox homeostasis genes are under control of both iron and copper master regulators.

Introduction

Iron (Fe) and copper (Cu) are essential trace metals that are required by plants for several aspects of redox chemistry. These metals form the active sites in numerous proteins involved in various processes, such as mitochondrial respiration, photosynthesis, ethylene perception, reactive oxygen species (ROS) protection, and other metabolic reactions [1-5]. For some metabolic functions, organisms may alternatively use Fe-containing proteins or Cu-containing proteins to catalyze biochemical reactions, depending on the bioavailability of each metal [4]. For example, some Fe-containing superoxide dismutases (FeSODs) can perform the same functions as some Cu-containing SODs (CuSODs), although they are products of different genes [3, 6-8].

Mineral deficiency or excess mineral supply can perturb normal physiology and metabolism in plants, resulting in abiotic stress and necessitating adjustments to mineral uptake. Both Fe and Cu uptake are largely controlled by transcriptional regulation. Fe homeostasis in *Arabidopsis thaliana* depends on the *FIT* gene [9], which is induced by Fe deficiency and encodes a bHLH family transcription factor. The FIT protein forms heterodimers with one of the subgroup-Ib bHLH proteins (bHLH38, bHLH39, bHLH100, bHLH101) [10, 11] and this heterodimer regulates the expression of a suite of Fe-regulated genes in roots. These genes include *FRO2*, which encodes a primary root ferric-chelate reductase gene [12], and *IRT1*, which encodes a root iron transporter [13, 14]. While *FIT* expression is limited to roots, the subgroup-Ib *bHLH* genes are also expressed in rosettes, where they are upregulated by Fe deficiency [15]. Cu homeostasis in Arabidopsis depends on the *SPL7* gene [16, 17], which is constitutively expressed and encodes a transcription factor that binds GTAC elements of promoters during Cu deficiency to activate expression of Cu-regulated genes. Included in the SPL7 regulon are Cu^{2+} reductases *FRO4* and *FRO5* [16], and the high-affinity Cu-transporter *COPT2*, which is involved in Cu uptake and Cu redistribution processes [18].

To cope with environmental stress due to deficiency or excess of nutrients, plants have crosstalk mechanisms to co-ordinate the uptake, chelation, transport, or regulatory mechanisms to maintain homeostasis. Cu deficiency can upregulate ferric-chelate reductase activity in roots [19-21], and simultaneous Fe and Cu deficiencies resulted in synergistic upregulation of Fe deficiency responses [22]. In addition to being regulated by Fe or Cu deficiencies individually, several metal homeostasis genes are responsive to both Fe and Cu deficiencies, such as *COPT2*, *ZIP2*, and the ferric-chelate reductase *FRO3* [15, 23-27]. These results indicate that there is crosstalk between Fe and Cu homeostasis within plants, however, a full catalog of genes that are regulated by Fe-Cu cross-talk and a clear picture of which genes are necessary for Fe-Cu crosstalk are not well-defined.

Some mechanisms of certain aspects Fe-Cu crosstalk have been described. Several Cu responsive genes and/or genes encoding Cu-containing proteins had altered expression under Fe deficiency in roots and rosettes of *Arabidopsis thaliana* [15, 25]. Additionally, Cu-responsive microRNAs (miRNAs) miR397 and miR398 changed in abundance under Fe deficiency [15]. Several mRNA targets of miRNA398, such as the Cu,Zn superoxide dismutases *CSD1* and *CSD2*, had increased abundance under Fe deficiency. The miR398s are upregulated under low Cu levels by SPL7 [17, 28], as is the Fe-SOD *FSD1*. The presence of miR398 results in degradation of *CSD*s. In Fe deficient *Arabidopsis thaliana*, miR398 abundance and expression of *FSD1* and *FSD2* decreased in rosettes, while expression of *CSD1* and *CSD2* increased [15]. These Fe-Cu crosstalk results suggested that a specific role for accumulation of Cu under Fe deficiency is for replacement of FeSOD proteins with CuSOD proteins, and inability to make this switch resulted in decreased ability to counteract ROS. Indeed, Cu concentrations were higher in Fe deficient leaves [15, 19, 21, 29]. Furthermore, under Fe deficiency, Cu accumulated in the rosettes of Arabidopsis prior to upregulation of Fe uptake genes [15, 25], suggesting that Cu uptake, in this growth condition, was regulated by Fe, but did not use the normal Fe uptake system. However, it remains unclear which genes may be responsible for Fe-deficiency stimulated Cu uptake. In a further example of Fe-Cu crosstalk, the

melon (*Cucumis melo*) iron uptake defective *fefe* mutant, with a lesion in a homolog of Arabidopsis *bHLH38* [30], can be rescued by growing the mutant plants under Cu deficiency, which stimulates Fe accumulation in the plants [31].

Ethylene production under Fe-deficiency is a well-known physiological response [32, 33] that at least partially regulates Fe uptake responses [34-36]. The ETHYLENE RESPONSE FACTOR (ERF) transcription factors contain AP2 domains and can act as activators or repressors of ethylene-responsive genes [37-39]. Most ERFs participate in ethylene-activated signaling pathways and intracellular signal transduction downstream of EIN3 and EIL1. The AP2/ERF family in *Arabidopsis* comprises 122 members in 12 groups. The biological functions of the majority of these genes are unknown, but many of the AP2/ERF genes that have been studied are involved in plant responses to abiotic stresses such as drought, cold, heat, salt, and hypoxia [40]. Arabidopsis *ERF4* and *ERF72* knockouts are less sensitive to Fe deficiency-induced chlorosis and have higher Fe uptake gene expression, suggesting that they are negative regulators of Fe responses [41, 42]. However, if or how other ERF genes are involved in Fe or Cu homeostasis is still unclear.

The overall purpose of this study was to increase our understanding of Fe-Cu crosstalk mechanisms by examining gene expression patterns and networks in Arabidopsis roots and rosettes treated with Fe deficiency, Cu deficiency, and simultaneous Fe and Cu deficiency. We test the hypothesis that Cu uptake is stimulated by Fe deficiency separately from Fe uptake, and is independent of normal Cu uptake mechanisms by using *spl7* mutants that lack normal Cu uptake gene expression. Our results suggest that Fe-deficiency-stimulated Cu uptake is *SPL7* independent, and also provide valuable insights into molecular genetic components associated with Fe-Cu crosstalk.

Materials and methods

Plant material and growing conditions

Seeds of *Arabidopsis thaliana* ecotype Col-0 and mutant *spl7* (SALK_109908c), *irt1* (SALK_054554c) and *fro2* (SALK_201379c) were obtained from the Arabidopsis Biological Resource Center (The Ohio State University). Seeds were imbibed in 0.1% agar at 4°C for 3d. Seeds were planted onto rockwool that was loosely packed into 1.5 ml centrifuge tubes with the bottoms removed. The tubes were inserted in lids of containers of nutrient solution, composed of: 0.8 mM KNO_3, 0.4 mM $Ca(NO_3)_2$, 0.3 mM $NH_4H_2PO_4$, 0.2 mM $MgSO_4$, 25 µM Fe(III)-EDDHA, 25 µM $CaCl_2$, 25 µM H_3BO_3, 2 µM $MnCl_2$, 2 µM $ZnSO_4$, 0.5 µM $CuSO_4$, 0.5 µM Na_2MoO_4, and 1 mM MES buffer (pH 5.5). Lighting was provided at a photoperiod of 16 h of 150 µmol m^{-2} s^{-1}, 4100K fluorescent light. After 10 d, seedlings were transferred to containers (4 plants per container) containing 0.75 liters of the same composition nutrient solution with constant aeration for an additional 14 d before plants were transferred to treatments. The pretreatment conditions for growing Col-0, *spl7*, *irt1* and *fro2* was 25 µM Fe and 0.1 µM Cu, and an additional 'rescue' pretreatment for *spl7* (which allowed *spl7* mutant plants to grow normally) was 25 µM Fe and 2.5 µM Cu. Pretreated plants were transferred to hydroponic media with 25 µM Fe or without Fe for 3 days, to test for alteration in rosette Cu concentration. In the *spl7* RNA-seq experiment, the plants were transferred from pretreatments into four treatments [25 µM Fe, 0.5 µM Cu (control); 25 µM Fe, 0 Cu (-Cu); 0 Fe, 0.5 µM Cu (-Fe); 0 Fe, 0 Cu (-Fe/-Cu)] for 3 days. The remaining mineral nutrients were at the same concentrations as described above. Three representative biological replicates of rosettes and roots were collected after 3 d of treatments and flash frozen in liquid nitrogen and stored at -80°C until use for further analysis.

Mineral analysis

Rosettes were dried at 60°C for at least 72 h before determining dry weight. Samples were digested with 3 ml of concentrated HNO_3 (VWR, West Chester, PA, USA, Trace metal grade) at room temperature overnight then at 100° C for 1.5 h, followed by addition of 2 ml of 30% H_2O_2 (Fisher Scientific, Fair Lawn, NJ, USA) and digestion for 1 h at 125° C, and finally heating the samples to dryness at 150° C. Dried samples were then resuspended in 3 ml of 1% HNO_3. Fe and Cu concentrations were determined by inductively coupled plasma-mass spectrometry (ICP-MS) at the University of Nebraska Redox Biology Spectroscopy and Biophysics Core.

Next generation RNA sequencing

Total RNA was isolated from roots and rosettes using the Plant RNeasy kit (Qiagen, Hilden, Germany). RNA quality and concentration was determined by UV spectrophotometry and by Agilent Bioanalyzer. RNA-sequencing was performed using an Illumina HiSeq 2000 instrument at the University of Nebraska Medical Center Next Generation Sequencing Core Facility. Barcoded libraries were constructed from 3 µg of root and rosette total RNA, with three biological replicate libraries per treatment. Replicates were run in separate lanes, with a total of six samples from different treatments in each lane. The short reads were deposited in NCBI's Gene Expression Omnibus and are accessible through GEO Series accession number GSE104916.

RNA-seq differential expression analysis

Each 101 bp RNA-seq read was trimmed using Trimmomatic [43] to make the average quality score larger than 30 and the minimum length 70 bp. All trimmed short reads were mapped to the *Arabidopsis thaliana* genome (version TAIR10) using TopHat [44], allowing up to two base mismatches per read. Reads mapped to multiple locations were discarded. Numbers of reads in genes were counted by the HTSeq-

count tool using corresponding *Arabidopsis thaliana* gene annotations (available from http://www-huber.embl.de/users/anders/HTSeq/). For pair-wise comparisons, significantly differentially expressed genes were identified by analyzing the numbers of reads aligned to genes with DEseq[45]. The thresholds for differential expression were fold-change > 1 (log2 scale) and adjusted *P*-values < 0.001 for the null hypothesis.

Bioinformatic analysis

The set of SPL7 responsive genes was determined by first performing several pairwise DEseq comparisons of *spl7* mutants to WT: 1) *spl7* grown under normal conditions (25 µM Fe and 0.1 µM Cu) to WT grown under normal conditions, 2) *spl7* 'rescue' plants (pre-treatment of 25 µM Fe and 2.5 µM Cu) to WT grown under normal conditions, 3) *spl7* 'rescue' plants compared to WT, both genotypes in -Fe treatment, 4) *spl7* 'rescue' plants compared to WT, both genotypes in -Cu treatment, and 5) *spl7* 'rescue' plants compared to WT, both genotypes in -Fe-Cu treatment. Sets of differentially expressed genes (DEGs) that were upregulated or downregulated in WT relative to *spl7* were compiled for both roots and rosettes. Genes that were differentially expressed in multiple conditions within roots or rosettes were retained in four sets (upregulated in WT roots, downregulated in WT roots, upregulated in WT rosettes, downregulated in WT rosettes). A Venn diagram of these sets was used to compile a list of 441 genes that was subsequently filtered by removing genes that were less than 2-fold (log2) higher or lower in WT relative to *spl7* mutants. This list was then compared to DEGs that responded to Fe deficiency, Cu deficiency, or simultaneous Fe and Cu deficiency within *spl7* or WT, and genes that did not respond to one of these treatments were removed. Finally, since SPL7 is known as a transcriptional activator, DEGs that were only in the root or rosette downregulated sets were removed if they responded only within a single treatment among -Fe, -Cu, or -Fe/-Cu treatments, in *spl7* or WT. These filtering steps left a list of 178 SPL7-responsive genes (Table S1).

Venn diagrams were used to compare different subsets of DEGs using Draw Venn Diagram (http://bioinformatics.psb.ugent.be/webtools/Venn/). DEGs from desired subsets were used as input for STRING database v10 (http://string-db.org) (Szklarczyk *et al*., 2015), using *Arabidopsis thaliana* as the organism, to identify known protein interactions and novel co-expressed networks. A combined STRING score of >0.7 (considered high confidence) was used in as a cutoff for subsequent visualization of networks. The text files (.tsv) from desired subsets were used as input for visualization of modules in Cytoscape v3.5.1 (http://www.cytoscape.org/) (Kohl *et al*., 2011). If a cluster of genes was not connected to another network, then it was considered a module. DAVID 6.8 database (Dennis *et al*., 2003) was used for non-redundant functional annotation clustering using TAIR-ID as the input, and *Arabidopsis thaliana* as the species, with EASE score (p-value) of <0.05 and minimum enrichment cut-off score of >1.3 with "high" as the classification stringency setting.

Results

spl7 mutant rescue by low Fe supply

Similar to previous reports [16, 17], *spl7* mutants grew poorly on normal Cu supply, with 49% lower rosette DW at 0.5 µM Cu and 89% lower DW at 0.1 µM Cu (Fig. 1a-c). Growth was restored when plants were supplied with 2.5 µM Cu (Fig. 1a). Surprisingly, rosette Cu concentration under normal Cu supply (0.5 µM) was only about 30% lower (Fig. 1d) than in WT. However, rosette Fe concentration was 37% higher at 0.5 µM Cu and 105% higher at 0.1 µM Cu (Fig. 1f). Based on this pattern, and because Cu deficiency can stimulate Fe uptake and recuse the *fefe* Fe uptake mutant phenotype [31], we hypothesized that Fe deficiency might stimulate Cu uptake and rescue the *spl7* mutant. Decreasing the Fe supply from 25 µM to 5 µM or 1 µM largely restored growth of *spl7* mutants on 0.5 µM or 0.1 µM Cu (Fig 1a, c), decreased their Fe concentration (Fig. 1f) while increasing Fe content to normal or near-normal (Fig. 1g). At 0.1 uM Cu supply, the Fe:Cu ratio (Fig. 2a) was 47 at 25 µM Fe, 27 at 5 µM Fe, and 18 at 1 µM Fe,

compared to ratios of 13-17 in WT plants in all treatments. These results indicate that *spl7*, in addition to being Cu deficient, tends to overaccumulate Fe in leaves. The results also indicate that Cu uptake induced by Fe deficiency is independent of *SPL7*, and is not likely to occur by the normal Cu uptake pathway. We recruited *fro2* and *irt1* Fe uptake mutants [12, 13] to test whether the normal Fe uptake pathway was required for this Fe deficiency-stimulated Cu accumulation. Like WT plants, both of these mutants were able to increase rosette Cu concentration by at least 2-fold (Fig. 2b) under Fe deficiency, indicating that the increased Cu accumulation under Fe deficiency did not occur through the normal Fe uptake pathway, and in WT plants is likely not a non-specific effect of increased Fe uptake gene expression.

Transcriptomic overview

Wilt-type and *spl7* mutant plants were grown as above (Fig. 1) before subjecting them to Fe, Cu, or simultaneous Fe and Cu deficiency treatments for 3d. The numbers of DEGs are presented in Table 1. The number of Fe-regulated genes in roots (832 in WT and 763 in *spl7*) was greater than the number of Cu-regulated genes (101 in WT and 149 in *spl7*), while simultaneous Fe and Cu deficiencies resulted in an intermediate number (341 in WT and 204 in *spl7*). In Fe-deficient rosettes, there were only 252 DEGs in WT compared to 775 in *spl7* mutants, while the numbers were similar for Cu responsive genes in rosettes of each genotype (122 in WT and 119 in *spl7*). Simultaneous Fe and Cu deficiencies resulted in greater DEG numbers in WT rosettes (583) than in *spl7* (244). The number of DEGs that responded to more than one mineral deficiency treatment ranged from 17-21% of the total number of differentially expressed genes (190/1056 for WT roots, 160/940 for *spl7* roots, 136/711 for WT rosettes, and 190/915 for *spl7* rosettes).

Fe regulon in WT and *spl7*

Since Fe deficiency stimulated Cu uptake in both WT and *spl7* plants (Fig. 1), we next determined the genes that responded to Fe deficiency in roots and rosettes of *spl7* and WT plants. In total, 1361 genes were differentially regulated under Fe deficiency in roots, of which 228 genes were common between *spl7* and WT (Fig. 3a and Dataset S1). Of these DEGs, 173 were upregulated under Fe deficiency in both genotypes, including several classical Fe deficiency response genes [25, 46] such as the subgroup Ib *bHLH* genes, *FRO2, IRT1, MYB10* and *MYB72,* and *NAS4* and also newly described *IMA3* (*FEP1*) [47, 48]. Similarly, known Fe responsive genes *bHLH38*, *bHLH39*, *bHLH100*, *bHLH101*, and *FRO3*, and all of the *IMA* genes were upregulated in rosettes in both genotypes (Fig. 3b), while Fe deficiency downregulated genes *FER1*, *FER3*, *FER4*, *YSL1*, and *NAS3* were downregulated in both genotypes. These results suggested that the *spl7* mutant has a largely intact Fe deficiency response.

Cu regulon in WT and *spl7*:

Since the *SPL7* gene is known to be necessary for normal regulation of Cu uptake, we determined DEGs under Cu-deficiency in roots and rosettes of WT and *spl7* plants from the 'rescue' pretreatment. In total from both genotypes, 240 genes were differentially expressed under Cu deficiency in roots, with little overlap between WT and *spl7* (Fig. 3c and Dataset S1). Several genes that are known SPL7 targets [16, 17] were upregulated in WT, but not in the *spl7* mutant, as expected. These included *ZIP2*, *FER1*, *CCH*, *FSD1*, *FRO4*, *FRO5*, *YSL2*, and *COPT2*. However, several known Fe deficiency-responsive genes were downregulated only in *spl7* mutant roots, including the four subgroup Ib *bHLH* genes, *FRO2*, *IRT1*, *IMA1* and *IMA2*, and *MYB10*. In rosettes (Fig. 3d), 215 genes were differentially expressed under Cu deficiency. Of these, the Fe-SOD gene *FSD1* was upregulated in both WT and *spl7*, while the Cu-SOD genes *CSD1* and *CSD2* were downregulated only in the *spl7* mutant. In rosettes, Cu-regulated genes *CSD1*, *CSD2*, and *FSD1* were differentially expressed only in WT, while *bHLH100* was

upregulated only in *spl7* mutants. *IMA1*, *2*, and *3* were downregulated in WT, but upregulated in *spl7* mutants.

Simultaneous Fe-Cu regulon in WT and *spl7*

When WT plants and *spl7* plants from the 'rescue' pretreatment were deprived of both Fe and Cu for three days, the many of the same DEGs from under single Fe or Cu deficiencies were detected (Fig. 3 and Dataset S1). However, the subsets in which they appeared were sometimes different than in the single deficiencies. In roots (Fig. 3e), the subgroup Ib *bHLH* genes, *FRO2*, and *IRT1* were differentially expressed only in WT, where they were downregulated, similar to results in Cu deficiency. The expression pattern of *IMA 1* and *2* also resembled that of roots under Cu deficiency. *FRO4*, *MYB10,* and *MYB72* were upregulated, but only in *spl7* mutants. In rosettes (Fig. 3f), *CSD2* was upregulated and *FSD1* was downregulated only in WT. Additionally, the subgroup Ib *bHLH* genes, *FRO3*, the *IMA* genes, and *NAS4* were upregulated, and *FER4*, *YSL1*, and *NAS3* were downregulated only in *spl7* mutants.

SPL7-responsive genes

While previous studies have determined sets of genes that had loss of normal regulation in *spl7* mutants (SPL7-responsive genes) under Cu deficiency or control conditions [16, 17], our additional treatments provided an opportunity to detect additional SPL7-responsive genes. By comparing DEGs in *spl7* mutants relative to WT in several conditions, we compiled a list of 178 SPL7-responsive genes (Table 2, Table S1). *SPL7* itself was included in the tables as a reference. Several known SPL7 targets were on the list, such as *FSD1*, *miR389c*, *ZIP2*, *YSL2*, and *COPT2*. All of these genes had higher transcripts in WT roots and/or rosettes than in *spl7* mutants in multiple conditions. Most of these SPL7-responsive genes were also downregulated in WT roots under Fe deficiency or upregulated in WT roots under Cu deficiency (or both), but normal regulation was lost in *spl7* mutants under these conditions. We also

noted several known Fe uptake genes were among the 178 SPL7-responsive genes, such as *IRT1*, *FRO2*, *bHLH38*, *bHLH39*, *bHLH100*, *bHLH101*, and *F6'H1*. Transcripts of these genes were mostly more abundant in WT roots relative to *spl7* in control and -Fe conditions, less abundant in WT roots relative to *spl7* under -Cu and -Fe-Cu conditions, and generally lower in WT rosettes under mineral deficiencies. In terms of differential expression by treatment, all of these genes were upregulated in Fe deficient WT roots, and fold-change in expression was similar in *spl7* mutants, except for the *bHLH* genes, where fold-changes were greater in *spl7*. In Cu deficient roots of WT, all of these Fe uptake genes were downregulated, whereas they were not differentially expressed in Cu deficient *spl7* roots, suggesting that *SPL7* is necessary to repress their expression under Cu deficiency. In simultaneous Fe and Cu deficient WT roots, the expression of these Fe uptake genes was downregulated, similar to that of Cu deficient roots, rather than being upregulated as in Fe deficient roots. However, in *spl7* mutants, the expression of these Fe uptake genes was upregulated, similar to that of Fe deficient WT roots, indicating that loss of *SPL7* also affects normal expression patterns under simultaneous Fe and Cu deficiencies. In Fe deficient rosettes, upregulation of most Fe uptake genes was much greater in *spl7* mutants than in WT. In rosettes of *spl7* mutants, the subgroup Ib *bHLH* genes were strongly upregulated under Cu or simultaneous Fe and Cu deficiencies, whereas they were not differentially expressed in WT rosettes under these conditions.

Identifying Fe-Cu crosstalk genes in WT and *spl7*

One of our objectives was to determine a catalog of genes that are regulated by Fe-Cu cross-talk using our treatments of roots and rosettes of WT and *spl7*. It is possible that because some genes are regulated differently in WT and *spl7*, for example upregulated by one treatment in WT but downregulated in *spl7*, the single treatment Venn series in Fig. 3 might miss some important cross-talk. To search within a larger set of relevant genes, we used a series of Venn diagrams (Fig. 4) to determine

the totality of DEGs in each genotype, for each tissue type. These steps were designed to move from specific treatments and expression changes to more general and broad categories that contained genes of interest, so that we could then analyze this set for enriched categories and specific patterns. First, four different three-way Venn diagrams for each tissue were used to attain a sum total DEGs within a genotype and also to visualize numbers of DEGs that occurred in one or more conditions. The sum of the genes in these sets (upregulated or downregulated, in WT or *spl7*, in roots or rosettes) were used as input for a four-way Venn; one each for roots and rosettes. The majority of these genes were found in only one outer subset which was upregulated and/or downregulated in only one genotype. These genes were considered to be of low interest. The central subsets (inside the red circle in Fig. 4) are considered to be potentially involved in Fe-Cu crosstalk. In roots, the inner sets contained 383 DEGs out of a total of 1607 DEGs, and for rosettes the inner sets contained 243 DEGs out of a total of 1383 DEGs. The final step was to compare the gene sets of interest in roots and rosettes, where 34 were found in both tissues, 349 were specific to roots, and 209 were specific to rosettes. The 383 and 243 DEGs (presented in Table S2) were then subjected to further GO enrichment analysis.

Functional annotation clustering of root and rosette regulated genes under simultaneous Fe and Cu deficiencies:

We performed DAVID functional annotation clustering of the 383 and 243 genes of interest above to identify enriched gene ontology (GO) terms in both roots and rosettes. There were 11 clusters in roots and six clusters in rosettes. In the roots, six biological process related clusters were enriched, which included ‘lipid transport’, ‘oxalate metabolic process’, ‘redox process’, ‘hydrogen peroxide catabolic process’, ‘flavonoid glucouronidation’ and ‘DNA templated transcription’ (Table S3). Four GO molecular function related clusters were enriched in roots, which included ‘serine-type carboxypeptidase activity’, ‘oxidoreductase activity’, ‘ATPase activity coupled to transmembrane

transport of substances' and 'protein-serine threonine kinase activity' (Table S3). A single GO cellular compartment category, 'integral component of the membrane' was enriched in roots which included the largest number of terms (n=50), compared to any other GO category.

In rosettes, two biological process clusters were enriched; 'DNA templated transcription' and 'xyloglucan metabolic process' (Table S3). There was a considerable overlap with respect to the GO terms in 'DNA templated transcription' in roots and rosettes. However, the enrichment score in rosettes (2.54) was higher than in roots (0.17). Two GO molecular function categories were enriched; 'iron ion binding' and 'calcium ion binding'. GO cellular compartment categories of 'integral part of the membrane' and 'plasma membrane' were enriched in rosettes.

Co-expression analysis of root and rosette regulated genes under Fe-Cu deficiency

To identify co-expressed genes and/or modules (networks) that are involved in Fe or Cu homeostasis in roots, we performed gene co-expression analysis of the 383 genes from Fig. 4 using the STRING-DB software. Nodes with evidence-based cutoff values of >0.7 combined score (high stringency) were visualized using Cytoscape, and modules representative of networks were further explored using STRING-DB to obtain GO enrichment. The root network (Fig. 5) comprised 120 nodes and 192 edges. The network was further divided into 12 modules, and two of these modules contained the majority of the nodes (74%). The largest module in roots consisted of 54 nodes and 95 edges (Fig. 5) and contained known Fe or Cu homeostasis genes, such as *IRT1*, *FRO2*, and the subgroup Ib *bHLH* genes. GO enrichment analysis of this module indicated that the biological processes 'iron ion homeostasis', 'response to external stimulus', 'response to stress' and 'cellular response to ethylene stimulus' were most enriched (Table S4). In the molecular function category, 'transcription factor activity, sequence-specific DNA binding', 'zinc ion transmembrane transporter activity' and 'monooxygenase activity' were

most enriched. The second largest module consisted of 35 nodes and 71 edges. GO enrichment analysis indicated that the biological processes 'response to decreased oxygen levels', 'response to abiotic stimulus', and 'oxidation-reduction processes' were most enriched.

The rosette network as determined by STRING-DB (Fig. 6) consisted of 96 nodes and 148 edges. The network was further divided into 17 modules, and five modules consisted of the majority of nodes (74%). The largest module in rosettes consisted of 34 nodes and 78 edges. GO enrichment analysis (Table S5) indicated that the biological processes 'response to oxygen containing compound', 'response to salicylic acid' and 'response to stress' were most enriched. In the molecular function category, 'calcium ion binding' and 'transcription factor activity, sequence-specific DNA binding' were most enriched. The second largest module consisted of 16 nodes which also contained known Fe-Cu homeostasis genes. GO enrichment analysis indicated that the biological processes 'iron ion homeostasis' and 'cellular response to stress' were enriched categories.

Iron deficiency-responsive ethylene related genes

Since the ethylene signaling pathway was enriched in certain subsets in this study, we further investigated the possibility of whether Cu regulation under Fe deficiency is affected by ethylene biosynthetic pathway or signaling related genes. In total, there were 49 DEGs associated with ethylene biosynthesis/ activated signaling pathway, combined across all subsets, tissues and genotypes (Table 4). Many of the ethylene signaling pathway genes were downregulated in WT compared to *spl7*, both in roots and rosettes. While several *ERF* family genes and ethylene biosynthetic genes were downregulated in WT, they were not differentially regulated in *spl7*. It is also notable that some AP2/ERF genes, including *RRTF1, DDF1, ERF13, ERF10,* and *DREB26* were upregulated in *spl7*, while they were either downregulated or not differentially regulated in WT under Fe deficiency.

Discussion

One purpose of this study was to increase our understanding of Fe-Cu crosstalk mechanisms by examining gene expression patterns and networks in Arabidopsis roots and rosettes treated with Fe deficiency, Cu deficiency, and simultaneous Fe and Cu deficiency. Upon compiling lists of genes of interest by various filtering strategies, it became clear that many of the genes involved in Fe-Cu crosstalk are already known as key players in Fe or Cu homeostasis. A substantial fraction of these genes are regulated by FIT, and even more are known to be regulated by SPL7, or were indicated to be SPL7-reponsive genes in this study, with a few of these genes being under control of both of these master regulators. Thus, both FIT and SPL7 contribute to Fe-Cu crosstalk. However, since many genes that were differentially expressed under Fe and Cu deficiency are not FIT or SPL7-responsive, there are likely other levels of regulation involved that cannot be identified from RNA-seq results alone. It is also possible that many of these genes were responding to alterations in metabolism due to Fe and/or Cu levels in the plant cells, rather than being directly regulated by mineral supply.

We tested the hypothesis that Cu uptake is stimulated by Fe deficiency separately from Fe uptake, and is independent of normal Cu uptake mechanisms by using *spl7* mutants. On normal nutrient solutions (25 µM Fe and 0.5 µM or 0.1 µM Cu), the *spl7* mutant had high leaf Fe:Cu ratio and grew poorly, but these parameters were restored by decreasing Fe supply. This growth rescue by manipulation of mineral supply is similar to previous results for the *fefe* Fe uptake mutant. The *fefe* mutant has high leaf Cu concentration and grows poorly on normal Fe and Cu supplies, but Cu deficiency stimulates Fe uptake and the plants begin to grow normally and have leaf Cu and Fe concentrations in the expected range [31]. The normal growth of *spl7* on 5 µM or lower Fe supply is similar to results of Bernal et al. (2012), where *spl7* mutants grew normally on 5 µM Fe and 0.25 µM Cu supply. Together, our *spl7* and *fefe* results demonstrate Fe-Cu crosstalk and show that whenever Cu or Fe uptake are

blocked, plants accumulate excessive concentrations of the other metal, and that lowering the supply of the excessive metal causes the plants to grow normally again.

In the case of *spl7* mutants, our RNA-seq results at least partially explained why Cu accumulation increased under Fe deficiency. In WT roots, SPL7 targets *COPT2* and *FRO4* were upregulated only under Cu deficiency, and this regulation did not occur in the *spl7* mutant. However, the *spl7* mutant roots had significantly higher expression of *COPT2* and *FRO4* under Fe deficiency and simultaneous Fe and Cu deficiency. Since *COPT2* is also a FIT target [9] and the FIT regulon appears to be regulated normally in *spl7* mutants (although at higher fold-change levels), FIT can upregulate *COPT2* (and other genes) when *SPL7* is not present. To date, the mechanisms of dual regulation of the several genes that are targets of both FIT and SPL7 have not been studied in detail.

Some of the most striking DEGs in this study include the subgroup Ib bHLHs; *bHLH38*, *bHLH39*, *bHLH100*, and *bHLH101*. These four genes always had similar expression patterns, suggesting that they are co-regulated. Most interestingly, under simultaneous Fe and Cu deficiency, Ib *bHLH* expression in WT roots resembled that of Cu deficiency in that they were downregulated, while an opposite pattern, with strong upregulation, occurred in *spl7* roots. In rosettes of WT, the subgroup Ib *bHLH* genes were strongly upregulated only under Fe deficiency, while upregulation was much stronger in the *spl7* mutant, and occurred not only under Fe deficiency but also under simultaneous Fe and Cu deficiency. Together, these results suggest that SPL7 could act directly or indirectly as a repressor of this class of *bHLH* genes. Our filtering criteria indicated that the Ib *bHLH* genes are among the SPL7-responsive genes. Several other known Fe uptake genes are included in this list, including *FRO2*, *IRT1*, and *F6'H1* [49, 50], which were also downregulated under Cu deficiency and simultaneous Fe and Cu deficiency. These Fe uptake genes are confirmed targets of FIT [9, 51]. *FIT* expression is activated in a *bHLH39* overexpression line [52], suggesting that the Fe uptake genes may be downstream of subgroup Ib *bHLH* genes activation. We also noted that the newly discovered *IMA/FEP* genes [47, 48] had a pattern of expression similar to that

of the subgroup Ib *bHLH* genes. The *IMA/FEP* genes encode small polypeptides that upregulate Fe uptake at the gene expression and physiological levels, and are upstream in the upregulation of the subgroup Ib *bHLH* genes. It is also noteworthy that the genes discussed above were contained in the Fe-Cu homeostasis-related modules of gene expression networks.

Previous studies of *spl7* mutants carried out to identify the SPL7 regulon [16, 17] did not identify the primary Fe uptake or regulatory genes discussed above as SPL7-dependent. However, these previous studies did not include Fe deficiency or simultaneous Fe and Cu deficiency treatments, which are where the lack of *SPL7* allowed its role to become apparent. To further determine whether SPL7 might directly repress these genes by binding to their promoters under Cu deficiency, we identified Cu response elements (GTAC) in the 3000 bp upstream of these and other genes. The numbers of GTAC elements in some known SPL7 targets are: *COPT2*, 3; *CCH*, 4; *FRO4*, 6; and *FSD1*, 11; while the numbers in some potential SPL7 targets are: *bHLH38*, 5; *bHLH39*, 6; *bHLH100*, 7; *bHLH101*, 8; *IMA1* and *IMA2*, 9; *IMA3*, 5; *WRKY40*, 4, and *RRTF1*, 7. While the presence of these GTAC elements does not conclusively show that SPL7 represses their expression, their identification leads to a testable hypothesis that we will address in future studies. Alternatively, SPL7 may indirectly repress the Ib *bHLH*, *IMA/FEP* genes, and other de-repressed genes by activating expression of an unidentified repressor that is not produced in *spl7* mutants.

The subgroup-Ib *bHLH* genes are also upregulated under Fe deficiency in rosettes [15, 53], where they were strongly upregulated by Fe deficiency in both WT and *spl7* mutants. However, since the FIT protein with which they interact in roots to upregulate Fe uptake genes is not expressed in leaves, the subgroup Ib bHLH proteins must be involved in regulating processes other than primary Fe uptake. It is possible that they interact with themselves, with each other, or with unknown proteins to upregulate other aspects of Fe homeostasis that occur in leaves. Some potential general roles for the subgroup IB

bHLHs are in rapid growth of leaf cells [54] and in regulation of ROS accumulation or signaling [55]. So far, no conclusive roles for Ib *bHLH* genes in leaf metal homeostasis have been established.

In addition to including several key Fe homeostasis genes, the gene co-expression networks we identified also included several AP2/ethylene response factors (*ERFs*). Many *ERFs* are downstream of EIN3 and EIL1 ethylene signaling proteins [37-39], which can also interact with FIT to stabilize the FIT protein [56]. Several of these *ERFs* respond to multiple stress conditions, such as cold, salt, and high light [40]. One transcription factor, *Redox Responsive Transcription Factor 1* (*RRTF1*), which was identified as both FIT- and SPL7-responsive in previous studies [16, 51], was downregulated in Fe-deficient WT roots but had the opposite response in *spl7* roots. This transcription factor gene was strongly downregulated in all mineral deficiency treatments in WT rosettes, but not in *spl7* rosettes, where it was upregulated under simultaneous Fe and Cu deficiencies. Targets of RRTF1 (e.g. *ERF6*, *RAP2.6*, *DDF1*, and *WRKY40*) are involved in regulating redox homeostasis [57, 58], and these genes had similar expression patterns (downregulated in WT and not differentially regulated or upregulated in *spl7*) and were present in the co-expression networks. WRKY40 is also required for full activation of *RRTF1* expression[58]. While the specific targets of many of these ERFs have not been determined, some of the ERFs are transcriptional repressors (e.g. ERF11) while others are activators. However, overexpression of *RRTF1* resulted in increased ROS production, while its inactivation resulted in less ROS accumulation [58]. Overexpression of another highly Fe and Cu responsive *AP2/ERF* gene, *DDF1*, resulted in decreased bioactive gibberellins and dwarfed plants [59], suggesting that lower *DDF1* expression might help to maintain growth. Mutants of Arabidopsis *ERF4* [41], *ERF72* [42], and apple *ERF4* [60] indicate that these proteins act as repressors of Fe deficiency responsive genes. However, that *ERF* genes are well known for roles in other stresses, and their especially strong downregulated response in WT leaves, suggest that their roles are not limited to regulating root Fe uptake. Thus, the lower expression of several *ERF* genes observed in this study

suggests a more general (but not necessarily less important) role in metal homeostasis and ROS production/scavenging rather than a role specifically in Fe-Cu cross-talk.

In conclusion, this study provided new insights into Fe -Cu crosstalk. We were able to identify gene expression patterns that explained why low Fe supply allowed *spl7* mutants to grow normally. Also, use of the *spl7* mutant under Fe deficiency and simultaneous Fe and Cu deficiency revealed potential new roles for SPL7 as a repressor of some aspects of Fe uptake, such as the *IMA*/*FEP* genes, subgroup Ib *bHLHs*, and the *ERF* redox homeostasis network. We have built a model (Fig. 7) that indicates the opposite effects of Fe and Cu deficiencies on the Fe uptake genes upstream of FIT, and the similar effects on the redox homeostasis network. Future studies will test critical aspects of this model.

Conflicts of Interest

There are no conflicts of interest to declare.

Acknowledgements

The authors thank Javier Seravalli for ICP-MS analysis. This project was partially supported by the Nebraska Agricultural Experiment Station with funding from the Hatch Act (Accession Number 22-375) through the USDA National Institute of Food and Agriculture, and by the National Science Foundation (NSF-IOS-1257568). The UNMC DNA Sequencing Core Facility receives partial support from the Nebraska Research Network In Functional Genomics NE-INBRE P20GM103427-14, The Molecular Biology of Neurosensory Systems CoBRE P30GM110768, The Fred & Pamela Buffett Cancer Center - P30CA036727, The Center for Root and Rhizobiome Innovation (CRRI) 36-5150-2085-20, and the Nebraska Research Initiative.

Supplementary material

Supplementary dataset 1. RNA-seq gene expression results for genes in Venn diagrams shown in Fig. 3.

Table S1. SPL7-responsive genes with fold change in abundance shown in *spl7* relative to WT and also within each genotype relative to the control treatment.

Table S2. Probable Fe-Cu crosstalk-related genes from central Venn diagram in Fig. 4.

Table S3. Enriched gene ontology (GO) terms in Fe-Cu crosstalk-related genes from central Venn diagram in Fig. 4 based on DAVID functional annotation clustering.

Table S4. GO enrichment analysis of co-expression network genes (Fig. 5) in roots as determined by STRING analysis.

Table S5. GO enrichment analysis of co-expression network genes (Fig. 5) in rosettes as determined by STRING analysis.

References

1. J. L. Burkhead, K. A. G. Reynolds, S. E. Abdel-Ghany, C. M. Cohu and M. Pilon, Copper homeostasis, *New Phytol.*, 2009, **182**, 799-816.
2. R. Hansch and R. R. Mendel, Physiological functions of mineral micronutrients (Cu, Zn, Mn, Fe, Ni, Mo, B, Cl), *Curr. Opin. Plant Biol.*, 2009, **12**, 259-266.
3. M. Pilon, K. Ravet and W. Tapken, The biogenesis and physiological function of chloroplast superoxide dismutases, *Biochimica Et Biophysica Acta-Bioenergetics*, 2011, **1807**, 989-998.
4. S. Puig, N. Andres-Colas, A. Garcia-Molina and L. Penarrubia, Copper and iron homeostasis in Arabidopsis: responses to metal deficiencies, interactions and biotechnological applications, *Plant Cell Environ.*, 2007, **30**, 271-290.
5. T. Hirayama, J. J. Kieber, N. Hirayama, M. Kogan, P. Guzman, S. Nourizadeh, J. M. Alonso, W. P. Dailey, A. Dancis and J. R. Ecker, RESPONSIVE-TO-ANTAGONIST1, a Menkes/Wilson disease–related copper transporter, is required for ethylene signaling in Arabidopsis, *Cell*, 1999, **97**, 383-393.
6. R. G. Alscher, N. Erturk and L. S. Heath, Role of superoxide dismutases (SODs) in controlling oxidative stress in plants, *J. Exp. Bot.*, 2002, **53**, 1331-1341.
7. D. J. Kliebenstein, R.-A. Monde and R. L. Last, Superoxide dismutase in Arabidopsis: An eclectic enzyme family with disparate regulation and protein localization, *Plant Physiol.*, 1998, **118**, 637-650.
8. F. Myouga, C. Hosoda, T. Umezawa, H. Iizumi, T. Kuromori, R. Motohashi, Y. Shono, N. Nagata, M. Ikeuchi and K. Shinozaki, A heterocomplex of iron superoxide dismutases defends chloroplast nucleoids against oxidative stress and is essential for chloroplast development in Arabidopsis, *The Plant Cell Online*, 2008, **20**, 3148-3162.
9. E. P. Colangelo and M. L. Guerinot, The essential basic helix-loop-helix protein FIT1 is required for the iron deficiency response., *The Plant Cell*, 2004, **16**, 3400-3412.

10. N. Wang, Y. Cui, Y. Liu, H. Fan, J. Du, Z. Huang, Y. Yuan, H. Wu and H.-Q. Ling, Requirement and functional redundancy of Ib subgroup bHLH proteins for iron deficiency responses and uptake in *Arabidopsis thaliana*, *Molecular plant*, 2013, **6**, 503-513.
11. Y. X. Yuan, H. L. Wu, N. Wang, J. Li, W. N. Zhao, J. Du, D. W. Wang and H. Q. Ling, FIT interacts with AtbHLH38 and AtbHLH39 in regulating iron uptake gene expression for iron homeostasis in *Arabidopsis*, *Cell Res.*, 2008, **18**, 385-397.
12. N. J. Robinson, C. M. Procter, E. L. Connolly and M. L. Guerinot, A ferric-chelate reductase for iron uptake from soils., *Nature*, 1999, **397**, 694-697.
13. G. Vert, N. Grotz, F. Dedaldechamp, F. Gaymard, M. L. Guerinot, J. F. Briat and C. Curie, IRT1, an Arabidopsis transporter essential for iron uptake from the soil and for plant growth, *Plant Cell*, 2002, **14**, 1223-1233.
14. D. Eide, M. Broderius, J. Fett and M. L. Guerinot, A novel iron-regulated metal transporter from plants identified by functional expression in yeast, *Proc. Natl. Acad. Sci. USA*, 1996, **93**, 5624-5628.
15. B. M. Waters, S. A. McInturf and R. J. Stein, Rosette iron deficiency transcript and microRNA profiling reveals links between copper and iron homeostasis in *Arabidopsis thaliana*, *J. Exp. Bot.*, 2012, **63**, 5903-5918.
16. M. Bernal, D. Casero, V. Singh, G. T. Wilson, A. Grande, H. Yang, S. C. Dodani, M. Pellegrini, P. Huijser, E. L. Connolly, S. S. Merchant and U. Krämer, Transcriptome sequencing identifies SPL7-regulated copper acquisition genes FRO4/FRO5 and the copper dependence of iron homeostasis in Arabidopsis, *The Plant Cell*, 2012, **24**, 738-761.
17. H. Yamasaki, M. Hayashi, M. Fukazawa, Y. Kobayashi and T. Shikanai, SQUAMOSA promoter binding protein-like7 is a central regulator for copper homeostasis in Arabidopsis, *The Plant Cell*, 2009, **21**, 347-361.
18. A. Perea-García, A. Garcia-Molina, N. Andrés-Colás, F. Vera-Sirera, M. A. Pérez-Amador, S. Puig and L. Peñarrubia, Arabidopsis copper transport protein COPT2 participates in the cross talk between iron deficiency responses and low-phosphate signaling, *Plant Physiol.*, 2013, **162**, 180-194.
19. V. Chaignon, D. Di Malta and P. Hinsinger, Fe-deficiency increases Cu acquisition by wheat cropped in a Cu-contaminated vineyard soil, *New Phytol.*, 2002, **154**, 121-130.
20. Y. X. Chen, J. Y. Shi, G. M. Tian, S. J. Zheng and Q. Lin, Fe deficiency induces Cu uptake and accumulation in *Commelina communis*, *Plant Science*, 2004, **166**, 1371-1377.
21. R. M. Welch, W. A. Norvell, S. C. Schaefer, J. E. Shaff and L. V. Kochian, Induction of iron(III) and copper(II) reduction in pea (*Pisum sativum* L.) roots by Fe and Cu staus: Does the root-cell plasmalemma Fe(III)-chelate reductase perform a general role in regulating cation uptake?, *Planta*, 1993, **1993**, 555-561.
22. F. J. Romera, V. M. Frejo and E. Alcántara, Simultaneous Fe- and Cu-deficiency synergically accelerates the induction of several Fe-deficiency stress responses in Strategy I plants, *Plant Physiol. Biochem.*, 2003, **41**, 821-827.
23. T. del Pozo, V. Cambiazo and M. González, Gene expression profiling analysis of copper homeostasis in *Arabidopsis thaliana*, *Biochem. Biophys. Res. Commun.*, 2010, **393**, 248-252.
24. V. Sancenon, S. Puig, I. Mateu-Andres, E. Dorcey, D. J. Thiele and L. Penarrubia, The Arabidopsis copper transporter COPT1 functions in root elongation and pollen development, *J. Biol. Chem.*, 2004, **279**, 15348-15355.
25. R. J. Stein and B. M. Waters, Use of natural variation reveals core genes in the transcriptome of iron-deficient *Arabidopsis thaliana* roots, *J. Exp. Bot.*, 2012, **63**, 1039-1055.

26. H. Wintz, T. Fox, Y. Y. Wu, V. Feng, W. Q. Chen, H. S. Chang, T. Zhu and C. Vulpe, Expression profiles of *Arabidopsis thaliana* in mineral deficiencies reveal novel transporters involved in metal homeostasis, *J. Biol. Chem.*, 2003, **278**, 47644-47653.
27. I. Mukherjee, N. H. Campbell, J. S. Ash and E. L. Connolly, Expression profiling of the Arabidopsis ferric chelate reductase (FRO) gene family reveals differential regulation by iron and copper, *Planta*, 2006, **223**, 1178-1190.
28. H. Yamasaki, S. E. Abdel-Ghany, C. M. Cohu, Y. Kobayashi, T. Shikanai and M. Pilon, Regulation of copper homeostasis by micro-RNA in Arabidopsis, *J. Biol. Chem.*, 2007, **282**, 16369-16378.
29. B. M. Waters and G. C. Troupe, Natural variation in iron use efficiency and mineral remobilization in cucumber (*Cucumis sativus*), *Plant Soil*, 2012, **352**, 185-197.
30. R. K. Ramamurthy and B. M. Waters, Mapping and characterization of the *fefe g*ene that controls iron iptake in melon (*Cucumis melo* L.), *Frontiers in Plant Science*, 2017, **8**.
31. B. M. Waters, S. A. McInturf and K. Amundsen, Transcriptomic and physiological characterization of the *fefe* mutant of melon (*Cucumis melo*) reveals new aspects of iron–copper crosstalk, *New Phytol.*, 2014, **203**, 1128-1145.
32. F. J. Romera, E. Alcantara and M. D. De la Guardia, Ethylene production by Fe-deficient roots and its involvement in the regulation of Fe-deficiency stress responses by strategy I plants, *Ann. Bot.*, 1999, **83**, 51-55.
33. B. M. Waters and D. G. Blevins, Ethylene production, cluster root formation, and localization of iron(III) reducing capacity in Fe deficient squash roots, *Plant Soil*, 2000, **225**, 21-31.
34. M. J. Garcia, C. Lucena, F. J. Romera, E. Alcantara and R. Perez-Vicente, Ethylene and nitric oxide involvement in the up-regulation of key genes related to iron acquisition and homeostasis in Arabidopsis, *J. Exp. Bot.*, 2010, **61**, 3885-3899.
35. C. Lucena, B. M. Waters, F. J. Romera, M. J. Garcia, M. Morales, E. Alcantara and R. Perez-Vicente, Ethylene could influence ferric reductase, iron transporter, and H+-ATPase gene expression by affecting FER (or FER-like) gene activity, *J. Exp. Bot.*, 2006, **57**, 4145-4154.
36. B. M. Waters, C. Lucena, F. J. Romera, G. G. Jester, A. N. Wynn, C. L. Rojas, E. Alcantara and R. Perez-Vicente, Ethylene involvement in the regulation of the H^+-ATPase *CsHA1* gene and of the new isolated ferric reductase *CsFRO1* and iron transporter *CsIRT1* genes in cucumber plants, *Plant Physiol. Biochem.*, 2007, **45**, 293-301.
37. M. Dubois, L. Van den Broeck and D. Inzé, The pivotal role of ethylene in plant growth, *Trends Plant Sci.*, 2018, **23**, 311-323.
38. F. Licausi, M. Ohme-Takagi and P. Perata, APETALA2/Ethylene Responsive Factor (AP2/ERF) transcription factors: mediators of stress responses and developmental programs, *New Phytol.*, 2013, **199**, 639-649.
39. M. Müller and S. Munné-Bosch, Ethylene response factors: a key regulatory hub in hormone and stress signaling, *Plant Physiol.*, 2015, **169**, 32-41.
40. U. J. Phukan, G. S. Jeena, V. Tripathi and R. K. Shukla, Regulation of Apetala2/Ethylene response factors in plants, *Frontiers in Plant Science*, 2017, **8**, 150.
41. W. Liu, N. J. U. Karemera, T. Wu, Y. Yang, X. Zhang, X. Xu, Y. Wang and Z. Han, The ethylene response factor AtERF4 negatively regulates the iron deficiency response in Arabidopsis thaliana, *PLOS ONE*, 2017, **12**, e0186580.
42. W. Liu, Q. Li, Y. Wang, T. Wu, Y. Yang, X. Zhang, Z. Han and X. Xu, Ethylene response factor AtERF72 negatively regulates Arabidopsis thaliana response to iron deficiency, *Biochem. Biophys. Res. Commun.*, 2017, **491**, 862-868.
43. A. M. Bolger, M. Lohse and B. Usadel, Trimmomatic: a flexible trimmer for Illumina sequence data, *Bioinformatics*, 2014, btu170.

44. C. Trapnell, A. Roberts, L. Goff, G. Pertea, D. Kim, D. R. Kelley, H. Pimentel, S. L. Salzberg, J. L. Rinn and L. Pachter, Differential gene and transcript expression analysis of RNA-seq experiments with TopHat and Cufflinks, *Nature protocols*, 2012, **7**, 562-578.
45. S. Anders and W. Huber, Differential expression analysis for sequence count data, *Genome biology*, 2010, **11**, R106.
46. W. Schmidt and T. J. Buckhout, A hitchhiker's guide to the Arabidopsis ferrome, *Plant Physiol. Biochem.*, 2011, **49**, 462-470.
47. L. Grillet, P. Lan, W. Li, G. Mokkapati and W. Schmidt, IRON MAN, a ubiquitous family of peptides that control iron transport in plants, *Nature Plants*, 2018, **(in press)**.
48. T. Hirayama, G. J. Lei, N. Yamaji, N. Nakagawa and J. F. Ma, The putative peptide gene FEP1 regulates iron deficiency response in Arabidopsis, *Plant Cell Physiol.*, 2018, DOI: 10.1093/pcp/pcy145, pcy145-pcy145.
49. N. B. Schmid, R. F. Giehl, S. Döll, H.-P. Mock, N. Strehmel, D. Scheel, X. Kong, R. C. Hider and N. von Wirén, Feruloyl-CoA 6′-Hydroxylase1-dependent coumarins mediate iron acquisition from alkaline substrates in arabidopsis, *Plant Physiol.*, 2014, **164**, 160-172.
50. H. Schmidt, C. Günther, M. Weber, C. Spörlein, S. Loscher, C. Böttcher, R. Schobert and S. Clemens, Metabolome Analysis of *Arabidopsis thaliana* Roots Identifies a Key Metabolic Pathway for Iron Acquisition, *PLoS ONE*, 2014, **9**, e102444.
51. H.-J. Mai, S. Pateyron and P. Bauer, Iron homeostasis in Arabidopsis thaliana: transcriptomic analyses reveal novel FIT-regulated genes, iron deficiency marker genes and functional gene networks, *BMC Plant Biol.*, 2016, **16**, 211.
52. M. A. Naranjo-Arcos, F. Maurer, J. Meiser, S. Pateyron, C. Fink-Straube and P. Bauer, Dissection of iron signaling and iron accumulation by overexpression of subgroup Ib bHLH039 protein, *Scientific Reports*, 2017, **7**, 10911.
53. H. Y. Wang, M. Klatte, M. Jakoby, H. Baumlein, B. Weisshaar and P. Bauer, Iron deficiency-mediated stress regulation of four subgroup Ib *BHLH* genes in *Arabidopsis thaliana*, *Planta*, 2007, **226**, 897-908.
54. M. E. Andriankaja, S. Danisman, L. F. Mignolet-Spruyt, H. Claeys, I. Kochanke, M. Vermeersch, L. De Milde, S. De Bodt, V. Storme, A. Skirycz, F. Maurer, P. Bauer, P. Mühlenbock, F. Van Breusegem, G. C. Angenent, R. H. Immink and D. Inzé, Transcriptional coordination between leaf cell differentiation and chloroplast development established by TCP20 and the subgroup Ib bHLH transcription factors, *Plant Mol. Biol.*, 2014, **85**, 233-245.
55. M. Noshi, N. Tanabe, Y. Okamoto, D. Mori, M. Ohme-Takagi, M. Tamoi and S. Shigeoka, Clade Ib basic helix-loop-helix transcription factor, bHLH101, acts as a regulatory component in photo-oxidative stress responses, *Plant Science*, 2018, **274**, 101-108.
56. S. Lingam, J. Mohrbacher, T. Brumbarova, T. Potuschak, C. Fink-Straube, E. Blondet, P. Genschik and P. Bauer, Interaction between the bHLH Transcription Factor FIT and ETHYLENE INSENSITIVE3/ETHYLENE INSENSITIVE3-LIKE1 Reveals Molecular Linkage between the Regulation of Iron Acquisition and Ethylene Signaling in Arabidopsis, *The Plant Cell Online*, 2011, **23**, 1815-1829.
57. A. Khandelwal, T. Elvitigala, B. Ghosh and R. S. Quatrano, Arabidopsis Transcriptome Reveals Control Circuits Regulating Redox Homeostasis and the Role of an AP2 Transcription Factor, *Plant Physiol.*, 2008, **148**, 2050-2058.
58. M. Matsuo, Joy M. Johnson, A. Hieno, M. Tokizawa, M. Nomoto, Y. Tada, R. Godfrey, J. Obokata, I. Sherameti, Yoshiharu Y. Yamamoto, F.-D. Böhmer and R. Oelmüller, High REDOX RESPONSIVE TRANSCRIPTION FACTOR1 Levels Result in Accumulation of Reactive Oxygen Species in Arabidopsis thaliana Shoots and Roots, *Molecular Plant*, 2015, **8**, 1253-1273.

59. H. Magome, S. Yamaguchi, A. Hanada, Y. Kamiya and K. Oda, *dwarf and delayed-flowering 1*, a novel *Arabidopsis* mutant deficient in gibberellin biosynthesis because of overexpression of a putative AP2 transcription factor, *The Plant Journal*, 2004, **37**, 720-729.

60. W. Liu, T. Wu, Q. Li, X. Zhang, X. Xu, T. Li, Z. Han and Y. Wang, An ethylene response factor (MxERF4) functions as a repressor of Fe acquisition in Malus xiaojinensis, *Scientific Reports*, 2018, **8**, 1068.

Figure Legends

Figure 1. Rescue of *spl7* mutants by low iron supply. a, Photograph of rosettes of WT (Col-0) and *spl7* mutants grown on Cu supply of 0, 0.5, 1.0, 2.5, or 5 µM with Fe supplied at 5 or 25 µM. b, Photograph of rosettes of WT (Col-0) and *spl7* mutants grown on Cu supply of 0.1 µM with Fe supplied at 1, 5, or 25 µM. c, Dry mass of rosettes of WT (Col) and *spl7* mutants grown as in A and B. d, rosette Cu concentration, e, rosette Cu content, f, rosette Fe concentration, and g, rosette Fe content of WT (Col) and *spl7* mutants grown as in A and B.

Figure 2. a, Rosette Fe:Cu ratio in WT (Col) and *spl7* mutants grown as in Fig. 1 plotted against rosette dry mass. Numbers near data points represent nutrient solution Cu and Fe concentrations (Cu/Fe) in µM. b, Rosette Cu concentration in WT (Col-0), *fro2* mutants, and *irt1* mutants grown with 25 µM Fe (+Fe) or without Fe (-Fe) for three days after a pre-treatment period with 25 µM Fe.

Figure 3. Venn diagrams of gene expression in WT and spl7 plants under single mineral deficiencies (-Fe or -Cu) and simultaneous Fe and Cu deficiency (-Fe-Cu) in roots and rosettes. a, Fe deficiency DEGs in roots; b, Fe deficiency DEGs in rosettes; c, Cu deficiency DEGs in roots; d, Cu deficiency DEGs in rosettes; e, simultaneous Fe and Cu deficiency DEGs in roots; f, simultaneous Fe and Cu deficiency DEGs in rosettes. Genes of interest known to be involved in Fe or Cu homeostasis are labeled in red, and indicated to the appropriate set in each diagram. Abbreviations: dn, downregulated; up, upregulated; s7, *spl7* mutant.

Figure 4. Venn diagram series used to isolate potential Fe-Cu crosstalk genes. Outer Venn diagrams on the upper half are genes from WT (left) and *spl7* (right) that were upregulated or downregulated in -Fe, -Cu, or -Fe-Cu treatments. Outer Venn diagrams on the lower half are genes from WT (left) and *spl7*

(right) that were upregulated or downregulated in -Fe, -Cu, or -Fe-Cu treatments. The center upper (roots) and lower (rosettes) Venn diagrams contain all genes that were upregulated or downregulated in any of the -Fe, -Cu, or -Fe-Cu treatments in WT or *spl7* mutants. The red circle shows genes that were advanced to the central Venn diagram that contains likely Fe-Cu crosstalk genes in roots and/or rosettes.

Figure 5. Gene co-expression networks in roots as determined by STRING analysis and visualized in Cytoscape. The largest module on the left was designated as the Fe-Cu crosstalk module of interest.

Figure 6. Gene co-expression networks in rosettes as determined by STRING analysis and visualized in Cytoscape. The second-largest module on the upper right was designated as the Fe-Cu crosstalk module of interest.

Figure 7. Model of roles of FIT and SPL7 in Fe-Cu crosstalk based on RNA-seq gene expression results. Transcription factors (FIT, bHLH Ib, SPL7, WRKY40, RRTF1) are represented as ovals; the peptides IMA/FEP are represented by a diamond, and downstream targets are represented by a green box. In this model, subgroup Ib bHLH proteins act upstream of and interact with FIT to activate Fe uptake target genes under Fe deficiency conditions. IMA/FEP peptides are upstream of subgroup Ib bHLH proteins. SPL7 protein represses (directly or indirectly) IMA/FEP and subgroup Ib bHLH expression under Cu deficiency and simultaneous Fe and Cu deficiency. SPL7 also represses WRKY40, which is upstream of RRTF1. RRTF1 is also a potential FIT target [51] and is repressed under Fe deficiency. WRKY40 and RRTF1 are upstream of the redox homeostasis network (see Table 2) which includes certain ERF proteins among others.

Table 1. Summary statistics of numbers of differentially expressed genes in WT or spl7 mutant roots or rosettes under Fe deficiency (-Fe), Cu deficiency (-Cu), or simultaneous Fe and Cu deficiencies (-Fe-Cu).

Treatment	Total	-Fe	-Cu	-Fe-Cu	Multiple	Multiple as % of total
WT root	1056	832	101	341	190	18.0
spl7 root	940	763	149	204	160	17.0
WT rosette	711	252	122	583	136	19.1
spl7 rosette	915	775	119	244	190	20.8

Table 2. Selected SPL7-responsive genes with fold change in abundance shown in *spl7* relative to WT and also within each genotype relative to the control treatment. The full table is presented in Table S1.

						Transcript abundance difference in spl7 relative to WT in each condition (log2 fold change, pairwise comparisons)								Fold-change (log2) within same genotype in each condition relative to +Fe+Cu condition											
						Roots	Roots	Roots	Roots	Shoots	Shoots	Shoots	Shoots	Roots	Roots	Roots	Roots	Roots	Roots	Shoots	Shoots	Shoots	Shoots	Shoots	Shoots
	elements	Gene name	Description	Fit regulated 1	SPL7 regulated 2	+Fe+Cu	-Fe	-Cu	-Fe-Cu	+Fe+Cu	-Fe	-Cu	-Fe-Cu	WT-Fe	WT-Cu	WT-Fe-Cu	spl7-Fe	spl7-Cu	spl7-Fe-Cu	WT-Fe	WT-Cu	WT-Fe-Cu	spl7-Fe	spl7-Cu	spl7-Fe-Cu
	AT5G18830	SPL7	squamosa promoter binding protein-like 7			-1.5	-1.5	-1.4	-1.4	-1.2	-1.2	-1.3	-1.2												
Previously known SPL7 responsive genes																									
	AT3G56240	CCH	copper chaperone	Yes	Yes	-1.2		-2.5	-1.2			-1.6			1.4					-1.1					
	AT3G46900	COPT2	copper transporter 2	Yes	Yes	-3.4		-4.8				-2.0	-1.7		2.0		2.6		2.4						
	AT5G38820		Transmembrane amino acid transporter family protein	Yes	Yes	-1.3	-1.8	3.2	4.0					2.1	-4.4	-2.3	1.6		2.9						
	AT4G29780		unknown protein	Yes	Yes	-1.1	1.4			-3.3		-1.7	1.4	-1.5		-1.7				-2.8	-1.5	-3.5	1.0		1.2
	AT1G47395	IMA2/FEP2	Iron Man/ Fe uptake Inducing peptide		Yes	-1.2	2.6	2.7	3.2	-5.1	3.8	3.9	3.1		-4.1	-2.2	4.7		2.2	3.1	-4.0		12.0	5.1	7.4
	AT1G52690		Late embryogenesis abundant protein (LEA) family protein		Yes					7.2		1.5		2.3			2.7						-6.9	-3.7	-7.4
	AT1G71200	CITF1	basic helix-loop-helix (bHLH) DNA-binding superfamily protein		Yes	-5.6		-7.2	-5.5						3.8										
	AT2G24850	TAT3	tyrosine aminotransferase 3		Yes	3.2		2.2		1.4		2.4	2.0						-2.3		-1.0	-1.2			
	AT2G29130	LAC2	laccase 2		Yes						2.0		1.3				-1.2				-1.2	-1.3	1.3	-1.6	
	AT2G47010		unknown protein		Yes	-1.3		-3.3				-1.3			1.4										
	AT3G28510		P-loop containing nucleoside triphosphate hydrolases superfamily protein		Yes		2.0		1.3		1.2	2.6	2.6	-1.7		-2.0						-2.7	2.1		
	AT3G57260	BGL2	beta-1,3-glucanase 2		Yes					2.0		2.3					3.0			1.7					-1.8
	AT4G10500		2-oxoglutarate (2OG) and Fe(II)-dependent oxygenase superfamily protein		Yes					2.6	1.4	3.3	1.3							1.9					-1.5
	AT4G25100	FSD1	Fe superoxide dismutase 1		Yes	-8.8	-5.0	-12.9	-12.1	-9.5	-7.5	-8.7	-8.8	-6.1	2.1					-5.5	1.3	-1.0		2.2	
	AT5G14565	MiR398c	mirna MIR398C		Yes	-5.7		-5.7						-5.8											
	AT5G22570	WRKY38	WRKY DNA-binding protein 38		Yes		1.9		1.3		1.6		3.1	-1.5		-2.2							1.6		
	AT5G23980	FRO4	ferric reduction oxidase 4		Yes	-5.6		-8.2	-3.3					-1.3	3.7		3.6		2.6				-1.0		
	AT5G24380	YSL2	YELLOW STRIPE like 2		Yes	-1.0		-2.4		-1.5		-2.7	-1.4		1.2					-1.1					
	AT5G57560	TCH4	Xyloglucan endotransglucosylase/hydrolase family protein		Yes	-1.0	1.4			-3.4	1.0	-2.5	1.2	-1.7						-2.4	-1.7	-3.2	2.0		1.5
	AT5G59520	ZIP2	ZRT/IRT-like protein 2		Yes	-3.6		-5.6	-3.3					-3.4	1.6										
Known Fe uptake genes																									
	AT4G19690	IRT1	iron-regulated transporter 1	Yes		-1.4	-1.3	2.9	3.7		2.0		2.0	2.0	-3.6	-2.8	2.0		2.3	1.4			2.7		
	AT1G01580	FRO2	ferric reduction oxidase 2	Yes		-1.2	-1.7	3.4	3.2		1.6			2.0	-3.9	-2.0	1.6		2.4				1.4		
	AT3G12900	F6'H1	2-oxoglutarate (2OG) and Fe(II)-dependent oxygenase superfamily protein	Yes		-2.0	-3.4	5.2	4.6					2.3	-7.0	-2.4			4.2						
	AT2G41240	bHLH100	basic helix-loop-helix protein 100			-1.2	1.1	2.7	4.4		5.2	6.5	6.5	2.7	-4.0	-3.2	5.1		2.4	4.1			14.5	6.5	9.1
	AT5G04150	bHLH101	basic helix-loop-helix (bHLH) DNA-binding superfamily protein BHLH101					1.8	3.3		3.6		2.5	1.3	-2.5	-2.1	2.4		1.6	1.5			7.4		4.5
	AT3G56970	bHLH38	basic helix-loop-helix (bHLH) DNA-binding superfamily protein					2.3	3.4		4.1		7.5	2.1	-3.4	-2.4	3.8		1.9	6.6			13.0		5.6
	AT3G56980	bHLH39	basic helix-loop-helix (bHLH) DNA-binding superfamily protein			-1.0			2.6		4.6		4.8	1.6	-1.5	-1.6	3.1		1.9	6.5			11.7		4.7
Fe or other metal homeostasis-related																									
	AT5G01600	FER1	ferretin 1				-2.0				-2.5		-2.5		1.2		-2.5		-1.3	-3.3		-1.7	-6.5		-4.9
	AT2G40300	FER4	ferritin 4								-2.4		-1.3				-1.8			-1.6			-4.4		-1.8
	AT5G26690		Heavy metal transport/detoxification superfamily protein								1.7		2.0	-1.9									2.3		
	AT1G47400	IMA1/FEP3	Iron Man/ Fe uptake Inducing peptide				2.1		3.0	-4.5	3.5	2.4	3.4		-4.1	-2.0	3.9		1.9	3.0	-2.5		10.9	4.4	7.0
	AT2G30766	IMA3/FEP1	Iron Man/ Fe uptake Inducing peptide							-4.8	2.0	3.2	3.1	4.5			5.4			2.8	-2.9		9.5	5.1	7.0
	AT1G21140		Vacuolar iron transporter (VIT) family protein				-2.9		1.1		-1.4		-1.2			-1.1	-2.3	1.0		-1.3			-3.4		-2.0
	AT3G18290	BTS	BRUTUS (BTS), a putative E3 ligase protein								2.2		1.2				1.4						3.3		1.7
Redox Homeostasis																									
	AT4G34410	RRTF1	redox responsive transcription factor 1	Yes		-2.5	4.2			-6.6		-3.2	7.7	-3.3		-3.1	3.4			-3.9	-2.7	-8.3			5.9
	AT1G80840	WRKY40	WRKY DNA-binding protein 40				1.9			-3.2		-1.4	2.7	-1.4		-1.4		1.1		-3.1	-2.1	-4.5			1.4
	AT1G12610	DDF1	DDF1/Integrase-type DNA-binding superfamily protein			-4.2	4.1			-6.6	-1.6		6.1	-3.1		-6.2	5.2			-2.1	-3.0	-7.4			5.2
	AT1G27730	ZAT10	salt tolerance zinc finger			-1.2	1.4	-1.1	-1.1	-2.1		-1.1	1.6	-1.9						-2.2	-1.6	-3.4			
	AT3G55980	SZF1	salt-inducible zinc finger 1							-2.3		-1.3		-1.5						-2.1	-1.5	-2.8			
	AT3G49620		2-oxoglutarate (2OG) and Fe(II)-dependent oxygenase superfamily protein			1.9	-1.9	3.6						1.2		-1.7	-2.5	1.2	-4.3						
	AT4G24570	DIC2	dicarboxylate carrier 2			-1.1	1.5		-1.3	-3.8	1.3	-1.9	1.4	-2.1						-3.2	-1.7	-3.7	1.9		1.5

Table 3. Gene expression of co-expression Fe-Cu modules of interest in roots and shoots of WT and *spl7* mutants as fold change in read counts in Fe deficiency (-Fe), Cu deficiency (-Cu), and simultaneous Fe and Cu deficiency (-Fe-Cu) tre

Roots																	
Module 1 Fe-Cu homeostasis related					Roots	Roots	Roots	Roots	Roots	Roots	Shoots	Shoots	Shoots	Shoots	Shoots	Shoots
Gene ID		**Description**	Fit regulated 1	SPL7 regulated 2	WT-Fe	WT-Cu	WT-Fe-Cu	spl7-Fe	spl7-Cu	spl7-Fe-Cu	WT-Fe	WT-Cu	WT-Fe-Cu	spl7-Fe	spl7-Cu	spl7-Fe-Cu
AT3G12900	F6'H1	2-oxoglutarate (2OG) and Fe(II)-dependent oxygenase superfamily protein	Yes	Yes	2.3	-7.0	-2.4			4.2						
AT1G01580	FRO2	ferric reduction oxidase 2	Yes	Yes	2.0	-3.9	-2.0	1.6		2.4				1.4		
AT4G19690	IRT1	iron-regulated transporter 1	Yes	Yes	2.0	-3.6	-2.8	2.0		2.3	1.4			2.7		
AT4G34410	RRTF1	redox responsive transcription factor 1	Yes	Yes	-3.3		-3.1	3.4			-3.9	-2.7	-8.3			5.9
AT5G38820		Transmembrane amino acid transporter family protein	Yes	Yes	2.1	-4.4	-2.3	1.6		2.9						
AT4G27654		unknown protein	Yes	Yes	-3.3			2.1			-4.0	-2.3	-5.8			4.5
AT4G31940	CYP82C4	cytochrome P450	Yes	Yes	1.4	-6.7	-3.1	1.1		4.2						
AT5G04150	bHLH101	basic helix-loop-helix (bHLH) DNA-binding superfamily protein BHLH101		Yes	1.3	-2.5	-2.1	2.4		1.6	1.5			7.4		4.5
AT3G56970	bHLH38	basic helix-loop-helix (bHLH) DNA-binding superfamily protein		Yes	2.1	-3.4	-2.4	3.8		1.9	6.6			13.0		5.6
AT3G56980	bHLH39	basic helix-loop-helix (bHLH) DNA-binding superfamily protein		Yes	1.6	-1.5	-1.6	3.1		1.9	6.5			11.7		4.7
AT2G41240	bHLH100	basic helix-loop-helix protein 100		Yes	2.7	-4.0	-3.2	5.1		2.4	4.1			14.5	6.5	9.1
AT1G47400	IMA1/FEP3	Iron Man/ Fe uptake Inducing peptide		Yes		-4.1	-2.0	3.9		1.9	3.0	-2.5		10.9	4.4	7.0
AT1G47395	IMA2/FEP2	Iron Man/ Fe uptake Inducing peptide		Yes		-4.1	-2.2	4.7		2.2	3.1	-4.0		12.0	5.1	7.4
AT5G05250		unknown protein		Yes		-1.6		2.9		1.3	1.3	-1.8		6.7	3.1	5.0
AT1G76650	CML38	calmodulin-like 38		Yes	-1.6			1.8	1.2		-2.8	-2.2	-3.7	-1.3		1.5
AT1G28370	ERF11	ERF domain protein 11		Yes	-1.1			1.5		-1.4	-3.3	-1.9	-4.5			
AT5G01600	FER1	ferretin 1		Yes		1.2		-2.5		-1.3	-3.3		-1.7	-6.5		-4.9
AT2G29460	GSTU4	glutathione S-transferase tau 4		Yes			-1.7	1.3	1.2	-2.9						
AT1G12610	DDF1	DDF1/Integrase-type DNA-binding superfamily protein		Yes	-3.1		-6.2	5.2			-2.1	-3.0	-7.4			5.2
AT1G80840	WRKY40	WRKY DNA-binding protein 40		Yes	-1.4		-1.4		1.1		-3.1	-2.1	-4.5			1.4
AT5G36890	BGLU42	beta glucosidase 42	Yes		1.4					1.6						
AT3G58060		Cation efflux family protein	Yes		3.1			3.0		2.6						
AT3G53280	CYP71B5	cytochrome p450	Yes		3.8					3.6						
AT3G07720		Galactose oxidase/kelch repeat superfamily protein	Yes		2.1	-1.3	-1.5			2.1						
AT4G19680	IRT2	iron regulated transporter 2	Yes		4.2			3.2		1.9						
AT1G52120		Mannose-binding lectin superfamily protein	Yes		4.8	1.6		3.0	1.7							
AT3G58810	MTPA2	metal tolerance protein A2	Yes		1.7	-1.5	-1.6	1.3		1.6						
AT1G56160	MYB72	myb domain protein 72	Yes		3.1			3.4		3.5						
AT5G55620		unknown protein	Yes		2.3					2.6						
AT3G25190		Vacuolar iron transporter (VIT) family protein	Yes				-1.2	-2.2								
AT2G32270	ZIP3	zinc transporter 3	Yes		-1.2			-1.1								
AT3G22910		ATPase E1-E2 type family protein					-1.8	1.6					-1.2			
AT1G74770	BTSL1	zinc ion binding BRUTUS-like			1.5	-1.0		1.7		1.1	3.9			4.6		
AT3G01830		Calcium-binding EF-hand family protein					-2.0	2.1			-1.3	-1.6	-4.0			
AT3G47480		Calcium-binding EF-hand family protein					-1.4	2.5								
AT1G73805		Calmodulin binding protein-like			-1.2		-1.1	1.1					-1.7	1.6		
AT5G42380	CML37	calmodulin like 37			-1.8		-1.4	2.0			-1.5	-2.1	-3.0			
AT5G26920		Cam-binding protein 60-like G			-1.0		-1.4	1.3								
AT3G26830	PAD3	cytochrome p450			1.0			2.0					-1.5			
AT2G30750	CYP71A12	cytochrome p450			1.6		-1.5	2.8	1.6							
AT3G26200	CYP71B22	cytochrome p450			2.6			2.1								
AT5G57220	CYP81F2	cytochrome p450					-1.0		1.3							
AT1G66090		Disease resistance protein (TIR-NBS class)					-1.3	2.2			-1.2	-1.7	-2.6			
AT5G47220	ERF2	ethylene responsive element binding factor 2			-1.0			1.4								
AT2G44840	ERF13	ethylene-responsive element binding factor 13			-1.8		-1.7	1.7		-1.3	-2.1	-1.3	-3.3			
AT1G26390		FAD-binding Berberine family protein			3.6			3.8								
AT1G56430	NAS4	nicotianamine synthase 4			2.2			5.1						3.4		1.6
AT2G26560	PLA2A	phospholipase A 2A			1.2		-1.2	1.2	1.2					1.4		
AT5G67370	DUF1230	Protein of unknown function (DUF1230)			2.1			4.7						2.5		
AT5G25260		SPFH/Band 7/PHB domain-containing membrane-associated protein family					-1.2	1.4	1.2							
AT5G38900		Thioredoxin superfamily protein					-1.2	1.5								
AT1G57630		Toll-Interleukin-Resistance (TIR) domain family protein					-1.1	1.9	1.1							
AT2G32140		transmembrane receptors					-1.2	1.6					-1.3			
AT1G25400		unknown protein					-1.1	1.3			-1.3	-1.4	-2.4	1.4		
Shoots					Roots	Roots	Roots	Roots	Roots	Roots	Shoots	Shoots	Shoots	Shoots	Shoots	Shoots
Module2-Fe-Cu homeostasis_related					WT-Fe	WT-Cu	WT-Fe-Cu	spl7-Fe	spl7-Cu	spl7-Fe-Cu	WT-Fe	WT-Cu	WT-Fe-Cu	spl7-Fe	spl7-Cu	spl7-Fe-Cu
AT4G19690	IRT1	iron-regulated transporter 1	Yes	Yes	2.0	-3.6	-2.8	2.0		2.3	1.4			2.7		
AT2G04050		MATE efflux family protein MATE efflux family protein	Yes	Yes				4.1			2.9			1.7		
AT5G04150	bHLH101	basic helix-loop-helix (bHLH) DNA-binding superfamily protein BHLH101		Yes	1.3	-2.5	-2.1	2.4		1.6	1.5			7.4		4.5
AT3G56970	bHLH38	basic helix-loop-helix (bHLH) DNA-binding superfamily protein		Yes	2.1	-3.4	-2.4	3.8		1.9	6.6			13.0		5.6
AT3G56980	bHLH39	basic helix-loop-helix (bHLH) DNA-binding superfamily protein		Yes	1.6	-1.5	-1.6	3.1		1.9	6.5			11.7		4.7
AT2G41240	bHLH100	basic helix-loop-helix protein 100		Yes	2.7	-4.0	-3.2	5.1		2.4	4.1			14.5	6.5	9.1
AT1G47400	IMA1/FEP3	Iron Man/ Fe uptake Inducing peptide		Yes		-4.1	-2.0	3.9		1.9	3.0	-2.5		10.9	4.4	7.0
AT1G47395	IMA2/FEP2	Iron Man/ Fe uptake Inducing peptide		Yes		-4.1	-2.2	4.7		2.2	3.1	-4.0		12.0	5.1	7.4
AT5G05250		unknown protein		Yes		-1.6		2.9		1.3	1.3	-1.8		6.7	3.1	5.0
AT4G25100	FSD1	Fe superoxide dismutase 1		Yes	-6.1	2.1					-5.5	1.3	-1.0		2.2	
AT5G01600	FER1	ferretin 1		Yes		1.2		-2.5		-1.3	-3.3		-1.7	-6.5		-4.9
AT3G49160		pyruvate kinase family protein		Yes							-2.4			-7.1		-2.4
AT1G23020	FRO3	ferric reduction oxidase 3						1.1			1.1			3.6		1.2
AT3G27060	TSO2	Ferritin/ribonucleotide reductase-like family protein									1.5			2.3		
AT3G07800		Thymidine kinase									1.7			1.1		
AT3G45730		unknown protein									1.8			1.7		

1, based on Colangelo and Guerinot, 2004 and Mai et al., 2016
2, Based on Yamasaki et al., 2009, Bernal et al., 2012, and Table 2

Table 4. Expression of ethylene biosynthesis or ethylene signalling pathway genes, based on DAVID classification, in Fe deficiency (-Fe), Cu deficiency (-Cu), and simultaneous Fe and Cu deficiency (-Fe-Cu) treatments relative to con

				Roots	Roots	Roots	Roots	Roots	Roots	Shoots	Shoots	Shoots	Shoots	Shoots	Shoots
Pathway_ID	**TAIR_ID**	**Gene_name**	**Description**	WT-Fe	WT-Cu	WT-Fe-Cu	spl7-Fe	spl7-Cu	spl7-Fe-Cu	WT-Fe	WT-Cu	WT-Fe-Cu	spl7-Fe	spl7-Cu	spl7-Fe-Cu
Ethylene Biosynthesis	AT1G01480	ACS2	1-amino-cyclopropane-1-carboxylate synthase 2	1.4			1.4								
Ethylene Biosynthesis	AT4G11280	ACS6	1-aminocyclopropane-1-carboxylic acid synthase 6	-1.1						-1.7	-1.2	-1.9			
Ethylene Biosynthesis	AT4G26200	ACS7	1-amino-cyclopropane-1-carboxylate synthase 7				2.5								
Ethylene signaling pathway	AT1G33760		Integrase-type DNA-binding superfamily protein							-4.9	-2.3	-6.9			
Ethylene signaling pathway	AT4G34410	RRTF1	redox responsive transcription factor 1	-3.3		-3.9	3.4			-3.9	-2.7	-8.3			5.9
Ethylene signaling pathway	AT1G77640		Integrase-type DNA-binding superfamily protein							-3.5	-1.9	-4.4			
Ethylene signaling pathway	AT1G28370	ERF11	ERF domain protein 11	-1.1			1.5		-1.4	-3.3	-1.9	-4.5			
Ethylene signaling pathway	AT4G25490	CBF1	C-repeat/DRE binding factor 1	-4.3						-3.0	-1.4	-2.2			
Ethylene signaling pathway	AT5G51990	CBF4	C-repeat-binding factor 4							-2.9		-4.7			
Ethylene signaling pathway	AT5G61600	ERF104	ethylene response factor 104	-1.6						-2.3		-3.2			
Ethylene signaling pathway	AT5G51190		Integrase-type DNA-binding superfamily protein	-2.3						-2.2	-1.2	-3.4			
Ethylene signaling pathway	AT2G44840	ERF13	ethylene-responsive element binding factor 13	-1.8		-1.7	1.7		-1.3	-2.1	-1.3	-3.3			
Ethylene signaling pathway	AT1G12610	DDF1	Integrase-type DNA-binding superfamily protein	-3.7		-6.2	5.2			-2.1	-3.0	-7.4			5.2
Ethylene signaling pathway	AT1G74930	ORA47	Integrase-type DNA-binding superfamily protein	-1.7						-1.8		-1.7			
Ethylene signaling pathway	AT4G25470	CBF2	C-repeat/DRE binding factor 2	-4.7						-1.7	-1.2	-1.3			
Ethylene signaling pathway	AT1G68840	RAV2	related to ABI3/VP1 2							-1.6	-1.2			-1.4	
Ethylene signaling pathway	AT4G17490	ERF6	ethylene responsive element binding factor 6							-1.5	-1.4	-3.4	1.7		
Ethylene signalling	AT2G38470	WRKY33	WRKY DNA-binding protein 33							-1.5	-1.3	-2.3			
Ethylene signaling pathway	AT1G21910	DREB26	Integrase-type DNA-binding superfamily protein				2.3			-1.4	-1.3	-1.8	1.8		
Ethylene signaling pathway	AT5G47230	ERF5	ethylene responsive element binding factor 5	-1.5						-1.3		-1.9			
Ethylene signaling pathway	AT1G44830		Integrase-type DNA-binding superfamily protein							-1.3					
Ethylene signaling pathway	AT3G15210	ERF4	ethylene responsive element binding factor 4							-1.2					
Ethylene signaling pathway	AT2G38340	DREB19	Integrase-type DNA-binding superfamily protein	1.6			2.3			2.5			2.7		
Ethylene signaling pathway	AT1G13260	RAV1	AP2/B3 domain transcription factor	-1.5											
Ethylene signaling pathway	AT5G47220	ERF2	ethylene responsive element binding factor 2	-1.4			1.4								
Ethylene signaling pathway	AT1G25560	TEM1	AP2/B3 transcription factor family protein	-1.3											
Ethylene signaling pathway	AT5G05410	DREB2A	DRE-binding protein 2A	-1.3								-1.7			
Ethylene signaling pathway	AT5G61590		Integrase-type DNA-binding superfamily protein	-1.2											
Ethylene signaling pathway	AT1G64380		Integrase-type DNA-binding superfamily protein	-1.2											
Ethylene signaling pathway	AT5G67190	DEAR2	DREB and EAR motif protein 2	-1.2											
Ethylene signaling pathway	AT4G17500	ERF-1	ethylene responsive element binding factor 1	-1.2									1.1		
Ethylene signaling pathway	AT1G73500	MKK9	MAP kinase kinase 9	-1.1											
Ethylene signaling pathway	AT4G36900	RAP2.10	related to AP2 10	-1.1											
Ethylene signaling pathway	AT1G77200		Integrase-type DNA-binding superfamily protein	1.2											
Ethylene signaling pathway	AT5G19790	RAP2.11	related to AP2 11	1.5											
Ethylene signaling pathway	AT5G13330	Rap2.6L	related to AP2 6l	1.9			1.4		-1.4						
Ethylene signaling pathway	AT5G64750	ABR1	Integrase-type DNA-binding superfamily protein				1.4								2.8
Ethylene signaling pathway	AT5G61890		Integrase-type DNA-binding superfamily protein				2.5								
Ethylene signaling pathway	AT5G44030	CESA4	cellulose synthase A4										1.5		
Ethylene signaling pathway	AT3G16770	EBP	ethylene-responsive element binding protein				1.8								
Ethylene signaling pathway	AT3G23240	ERF1	ethylene response factor 1					1.4	-1.1						
Ethylene signaling pathway	AT1G03800	ERF10	ERF domain protein 10				2.5								
Ethylene signaling pathway	AT2G47520	ERF71	Integrase-type DNA-binding superfamily protein			3.4	7.1	4.8					5.5		
Ethylene signaling pathway	AT5G40990	GLIP1	GDSL lipase 1				2.5								
Ethylene signaling pathway	AT4G18780	IRX1	cellulose synthase family protein										1.6		
Ethylene signaling pathway	AT4G00416	MBD3	methyl-CPG-binding domain 3				5.8								

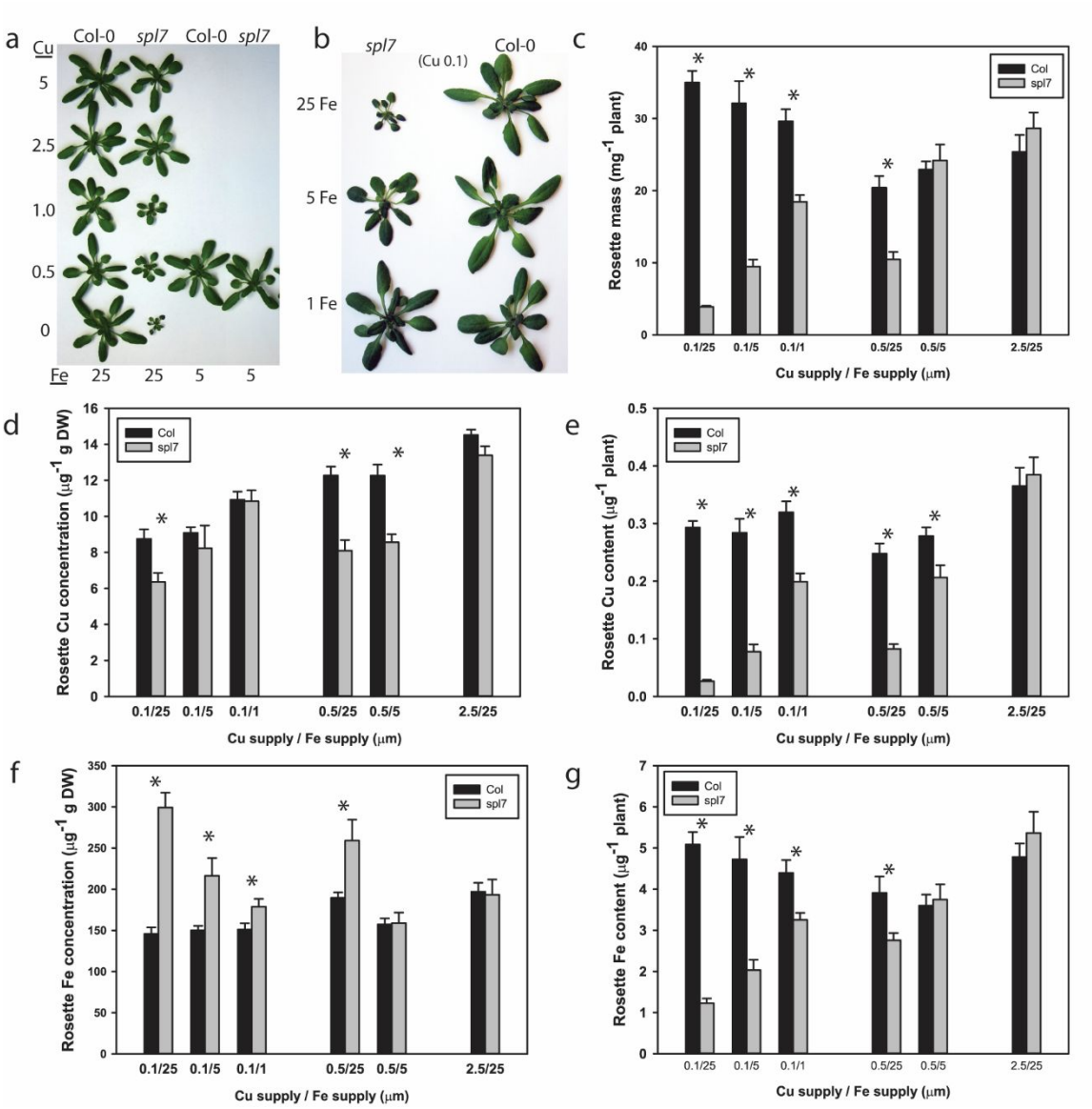

Figure 1. Rescue of *spl7* mutants by low iron supply. a, Photograph of rosettes of WT (Col-0) and *spl7* mutants grown on Cu supply of 0, 0.5, 1.0, 2.5, or 5 µM with Fe supplied at 5 or 25 µM. b, Photograph of rosettes of WT (Col-0) and *spl7* mutants grown on Cu supply of 0.1 µM with Fe supplied at 1, 5, or 25 µM. c, Dry mass of rosettes of WT (Col) and *spl7* mutants grown as in A and B. d, rosette Cu concentration, e, rosette Cu content, f, rosette Fe concentration, and g, rosette Fe content of WT (Col) and *spl7* mutants grown as in A and B.

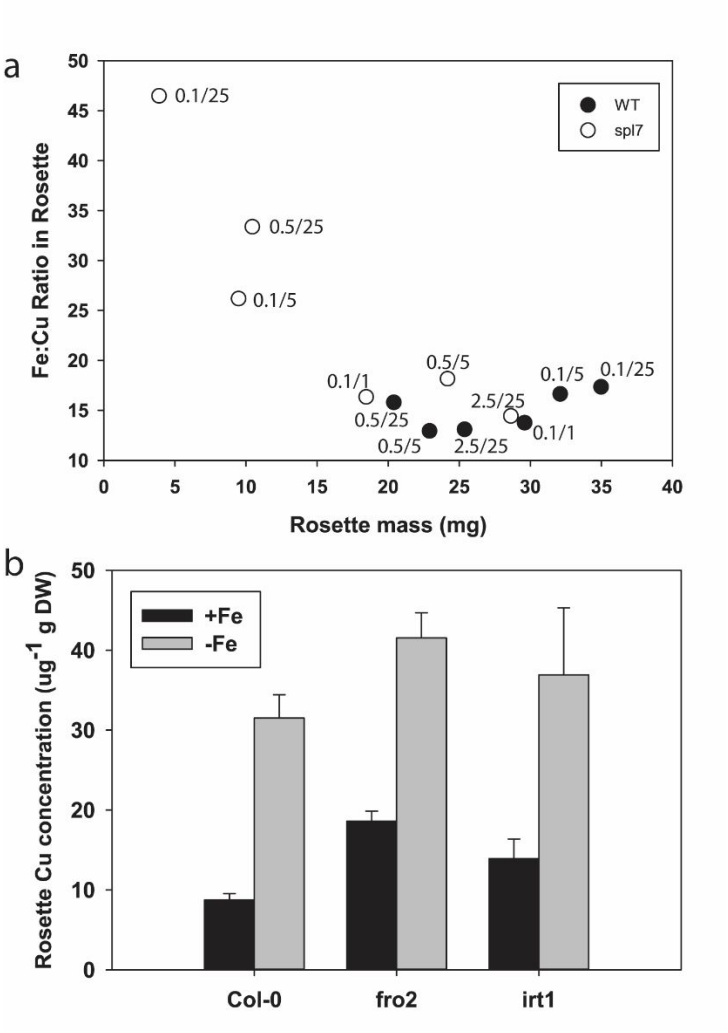

Figure 2. a, Rosette Fe:Cu ratio in WT (Col) and *spl7* mutants grown as in Fig. 1 plotted against rosette dry mass. Numbers near data points represent nutrient solution Cu and Fe concentrations (Cu/Fe) in µM. b, Rosette Cu concentration in WT (Col-0), *fro2* mutants, and *irt1* mutants grown with 25 µM Fe (+Fe) or without Fe (-Fe) for three days after a pre-treatment period with 25 µM Fe.

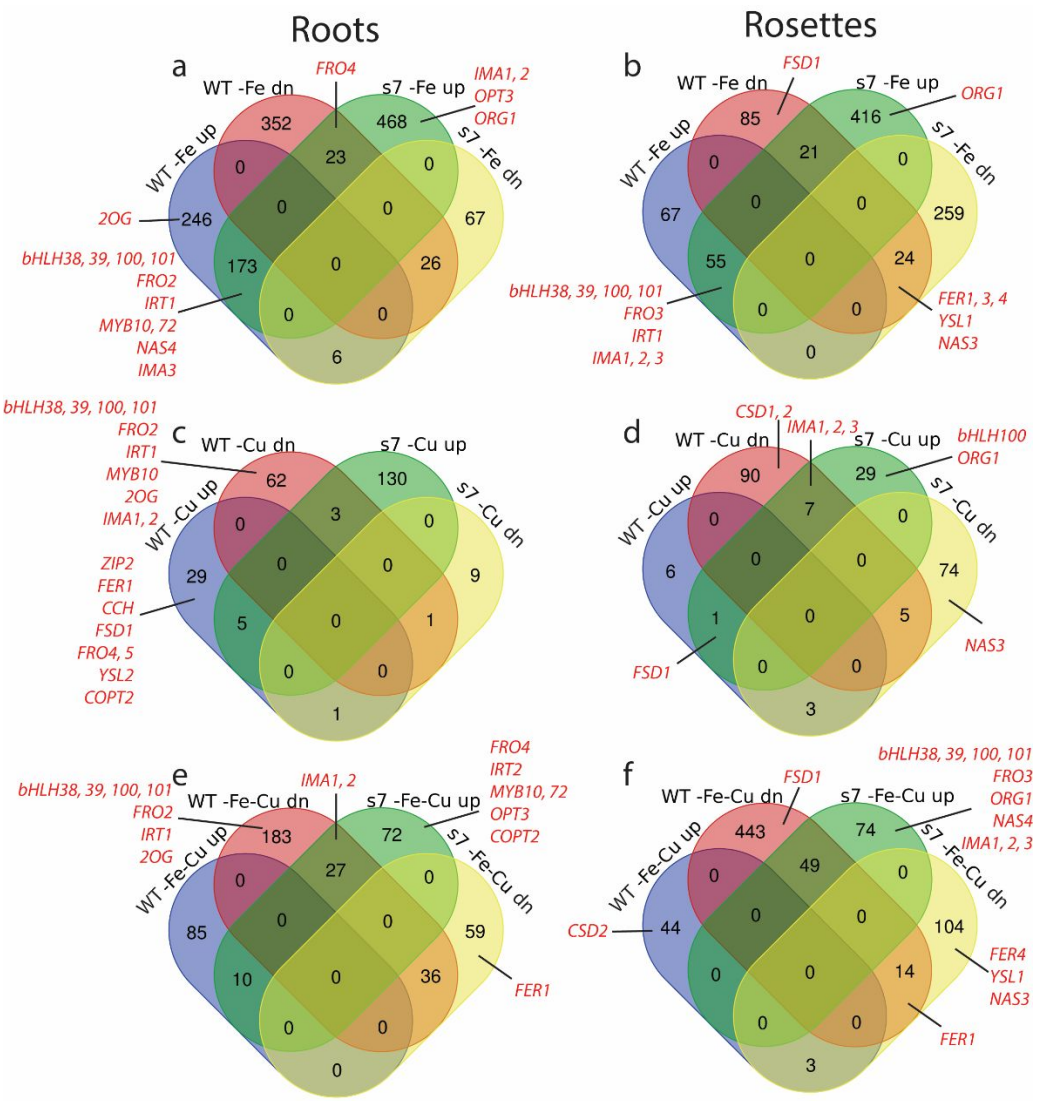

Figure 3. Venn diagrams of gene expression in WT and spl7 plants under single mineral deficiencies (-Fe or -Cu) and simultaneous Fe and Cu deficiency (-Fe-Cu) in roots and rosettes. a, Fe deficiency DEGs in roots; b, Fe deficiency DEGs in rosettes; c, Cu deficiency DEGs in roots; d, Cu deficiency DEGs in rosettes; e, simultaneous Fe and Cu deficiency DEGs in roots; f, simultaneous Fe and Cu deficiency DEGs in rosettes. Genes of interest known to be involved in Fe or Cu homeostasis are labeled in red, and indicated to the appropriate set in each diagram. Abbreviations: dn, downregulated; up, upregulated; s7, *spl7* mutant.

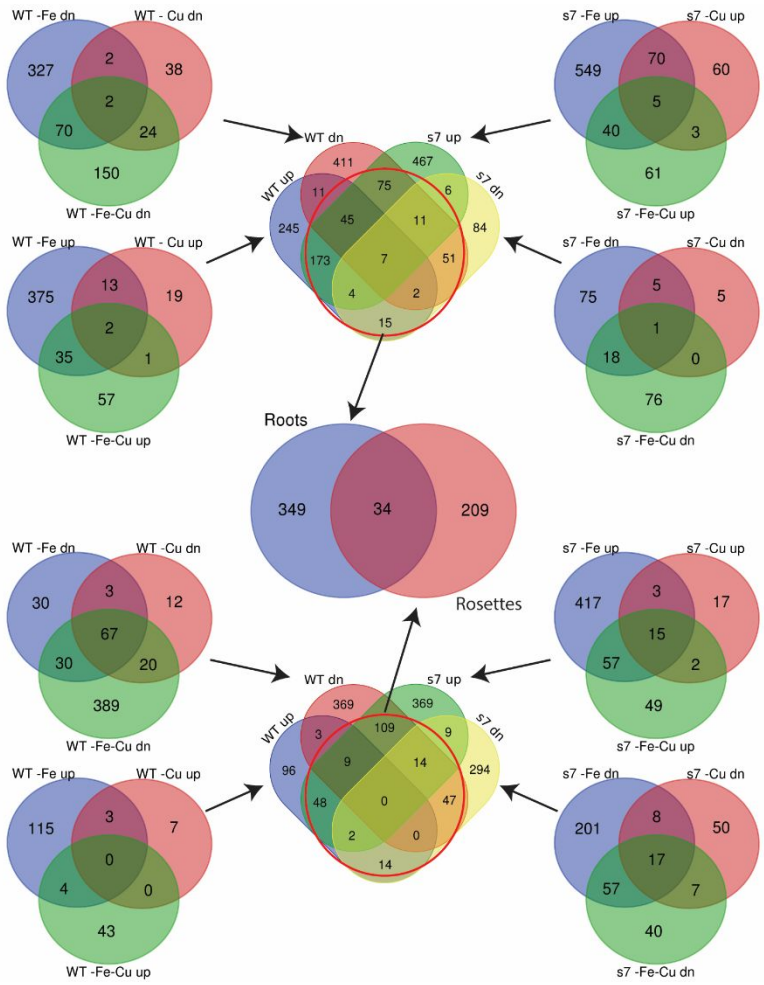

Figure 4. Venn diagram series used to isolate potential Fe-Cu crosstalk genes. Outer Venn diagrams on the upper half are genes from WT (left) and *spl7* (right) that were upregulated or downregulated in -Fe, -Cu, or -Fe-Cu treatments. Outer Venn diagrams on the lower half are genes from WT (left) and *spl7* (right) that were upregulated or downregulated in -Fe, -Cu, or -Fe-Cu treatments. The center upper (roots) and lower (rosettes) Venn diagrams contain all genes that were upregulated or downregulated in any of the -Fe, -Cu, or -Fe-Cu treatments in WT or *spl7* mutants. The red circle shows genes that were advanced to the central Venn diagram that contains likely Fe-Cu crosstalk genes in roots and/or rosettes.

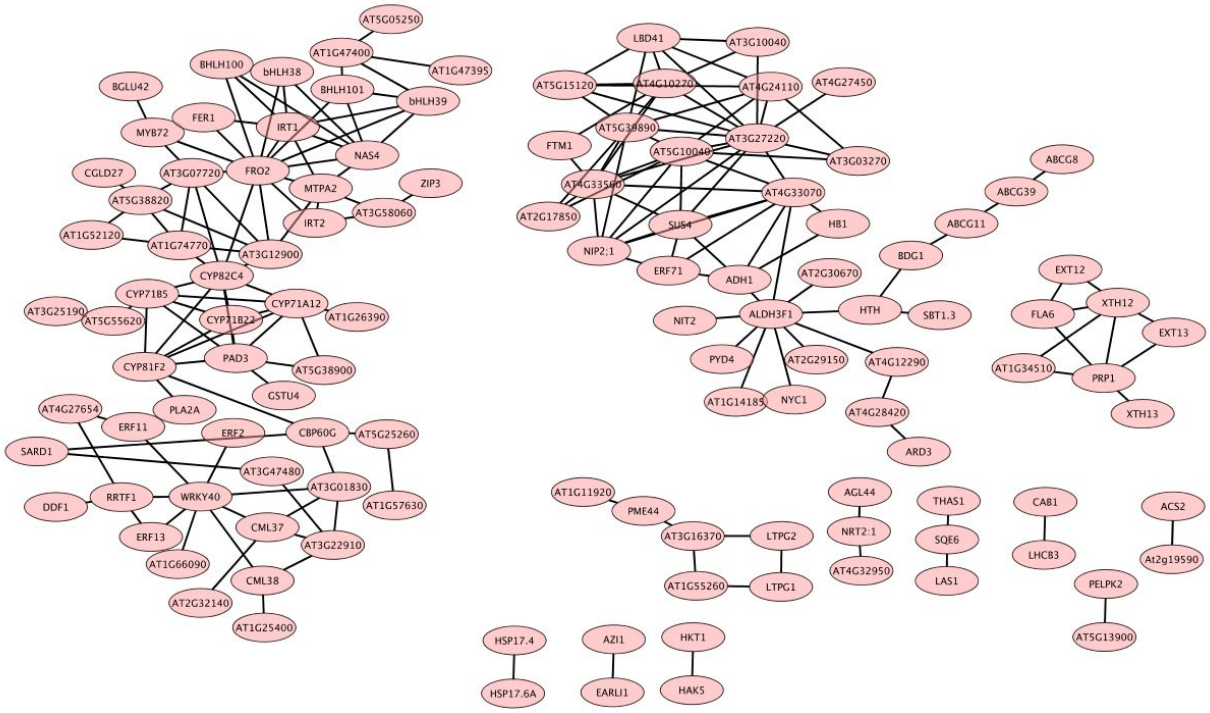

Figure 5. Gene co-expression networks in roots as determined by STRING analysis and visualized in Cytoscape. The largest module on the left was designated as the Fe-Cu crosstalk module of interest.

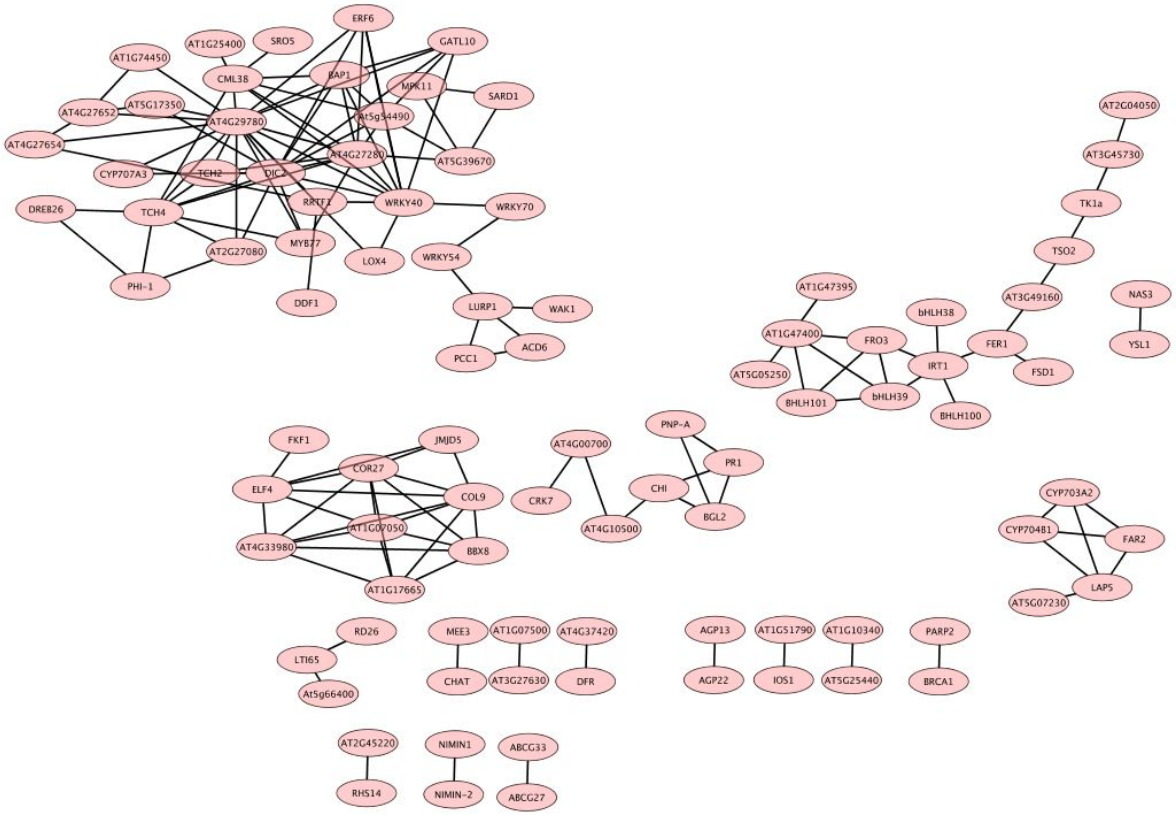

Figure 6. Gene co-expression networks in rosettes as determined by STRING analysis and visualized in Cytoscape. The second-largest module on the upper right was designated as the Fe-Cu crosstalk module of interest.

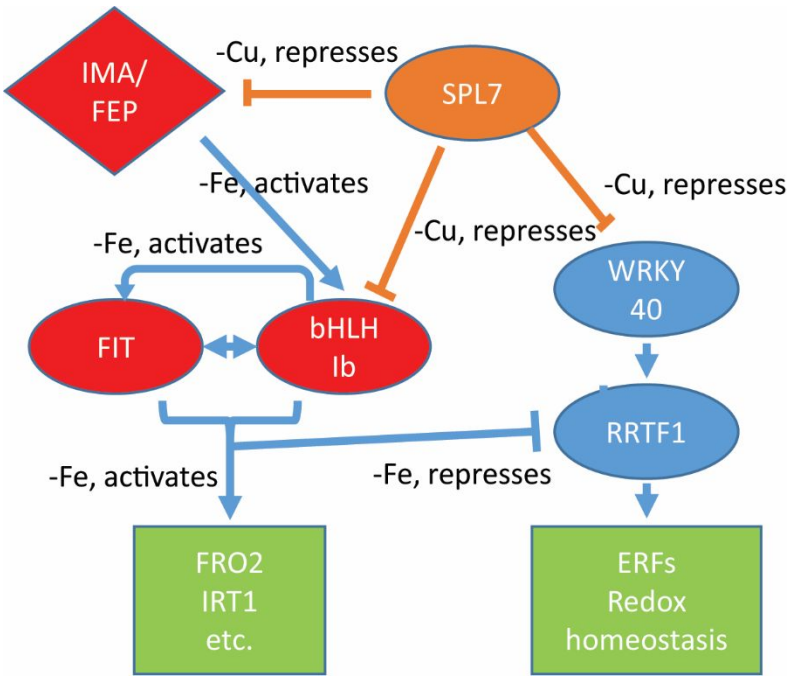

Figure 7. Model of roles of FIT and SPL7 in Fe-Cu crosstalk based on RNA-seq gene expression results. Transcription factors (FIT, bHLH Ib, SPL7, WRKY40, RRTF1) are represented as ovals; the peptides IMA/FEP are represented by a diamond, and downstream targets are represented by a green box. In this model, subgroup Ib bHLH proteins act upstream of and interact with FIT to activate Fe uptake target genes under Fe deficiency conditions. IMA/FEP peptides are upstream of subgroup Ib bHLH proteins. SPL7 protein represses (directly or indirectly) IMA/FEP and subgroup Ib bHLH expression under Cu deficiency and simultaneous Fe and Cu deficiency. SPL7 also represses WRKY40, which is upstream of RRTF1. RRTF1 is also a potential FIT target [51] and is repressed under Fe deficiency. WRKY40 and RRTF1 are upstream of the redox homeostasis network (see Table 2) which includes certain ERF proteins among others.

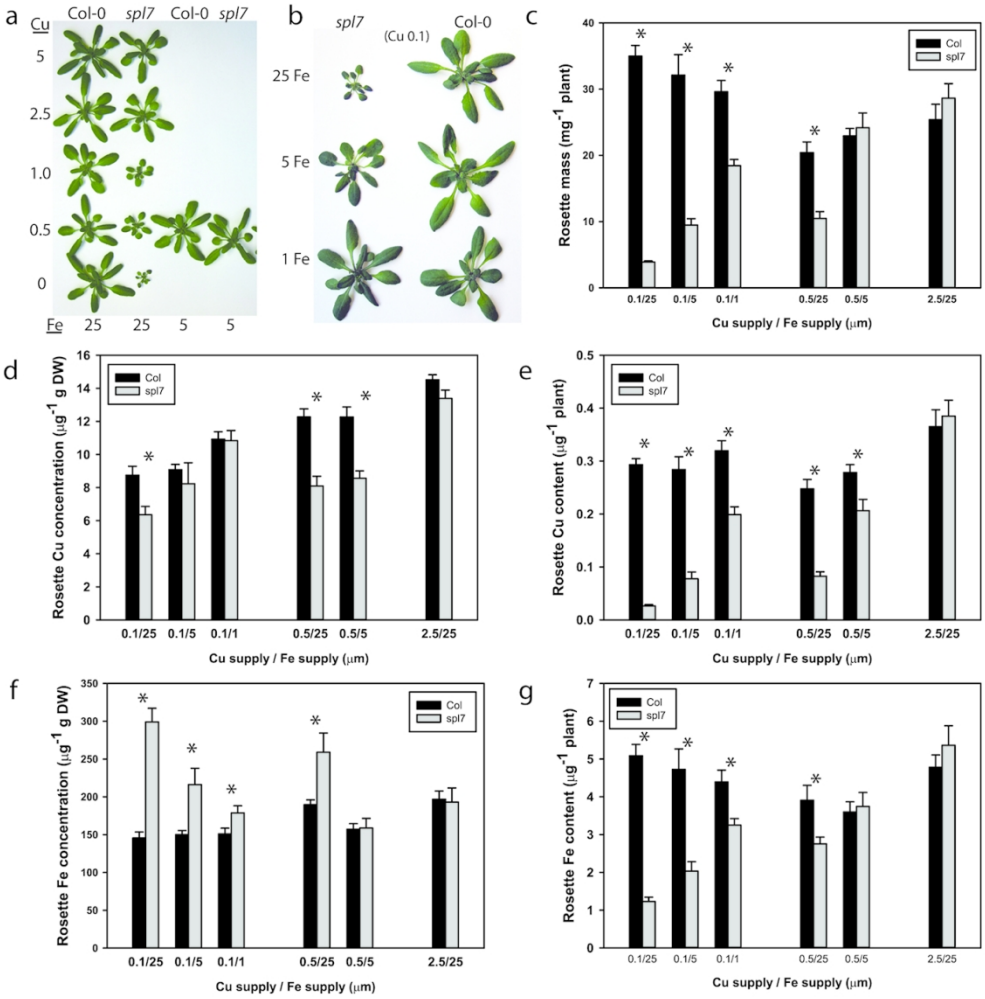

Figure 1. Rescue of spl7 mutants by low iron supply. a, Photograph of rosettes of WT (Col-0) and spl7 mutants grown on Cu supply of 0, 0.5, 1.0, 2.5, or 5 μM with Fe supplied at 5 or 25 μM. b, Photograph of rosettes of WT (Col-0) and spl7 mutants grown on Cu supply of 0.1 μM with Fe supplied at 1, 5, or 25 μM. c, Dry mass of rosettes of WT (Col) and spl7 mutants grown as in A and B. d, rosette Cu concentration, e, rosette Cu content, f, rosette Fe concentration, and g, rosette Fe content of WT (Col) and spl7 mutants grown as in A and B.

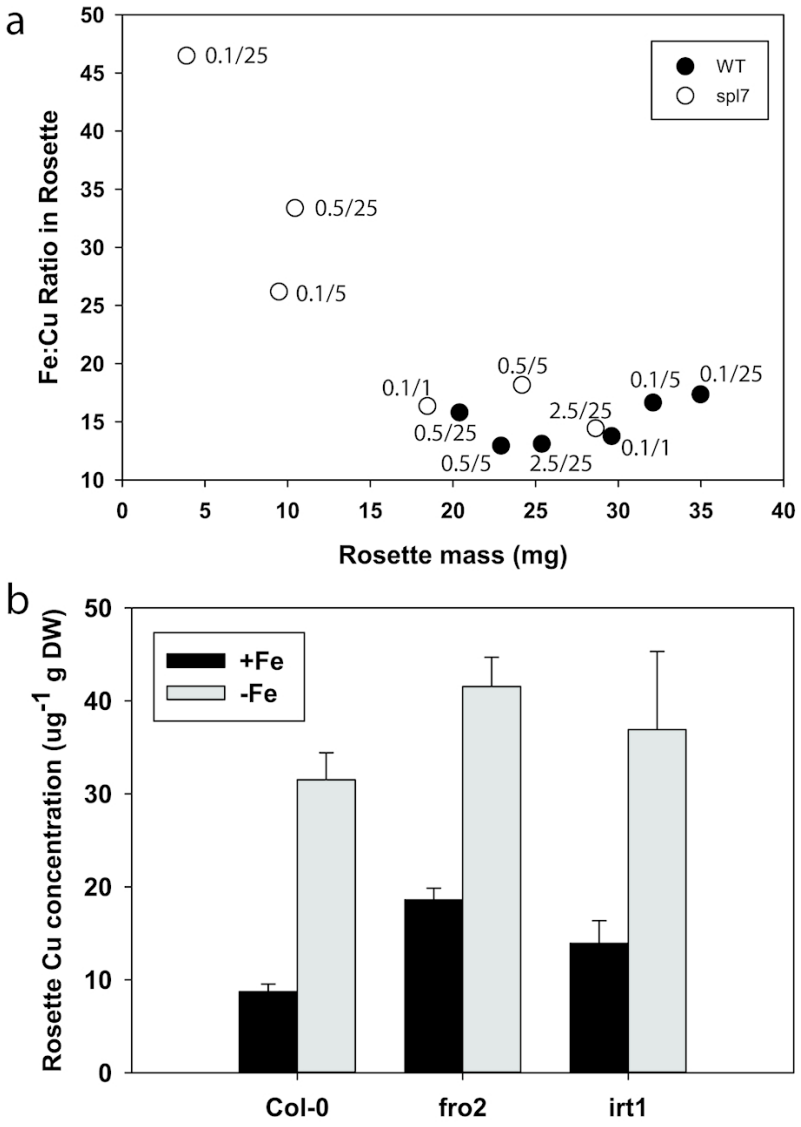

Figure 2. a, Rosette Fe:Cu ratio in WT (Col) and spl7 mutants grown as in Fig. 1 plotted against rosette dry mass. Numbers near data points represent nutrient solution Cu and Fe concentrations (Cu/Fe) in μM. b, Rosette Cu concentration in WT (Col-0), fro2 mutants, and irt1 mutants grown with 25 μM Fe (+Fe) or without Fe (-Fe) for three days after a pre-treatment period with 25 μM Fe.

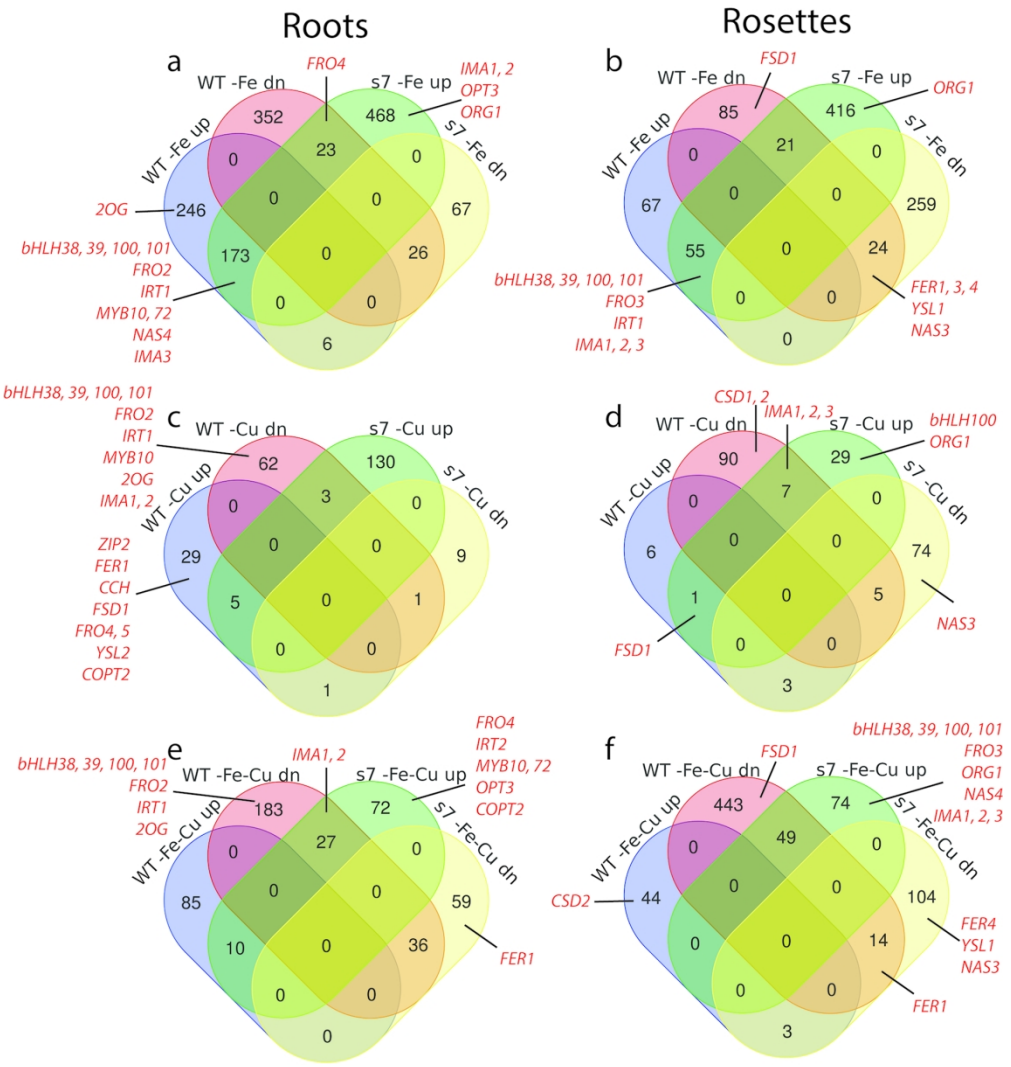

Figure 3. Venn diagrams of gene expression in WT and spl7 plants under single mineral deficiencies (-Fe or -Cu) and simultaneous Fe and Cu deficiency (-Fe-Cu) in roots and rosettes. a, Fe deficiency DEGs in roots; b, Fe deficiency DEGs in rosettes; c, Cu deficiency DEGs in roots; d, Cu deficiency DEGs in rosettes; e, simultaneous Fe and Cu deficiency DEGs in roots; f, simultaneous Fe and Cu deficiency DEGs in rosettes. Genes of interest known to be involved in Fe or Cu homeostasis are labeled in red, and indicated to the appropriate set in each diagram. Abbreviations: dn, downregulated; up, upregulated; s7, spl7 mutant.

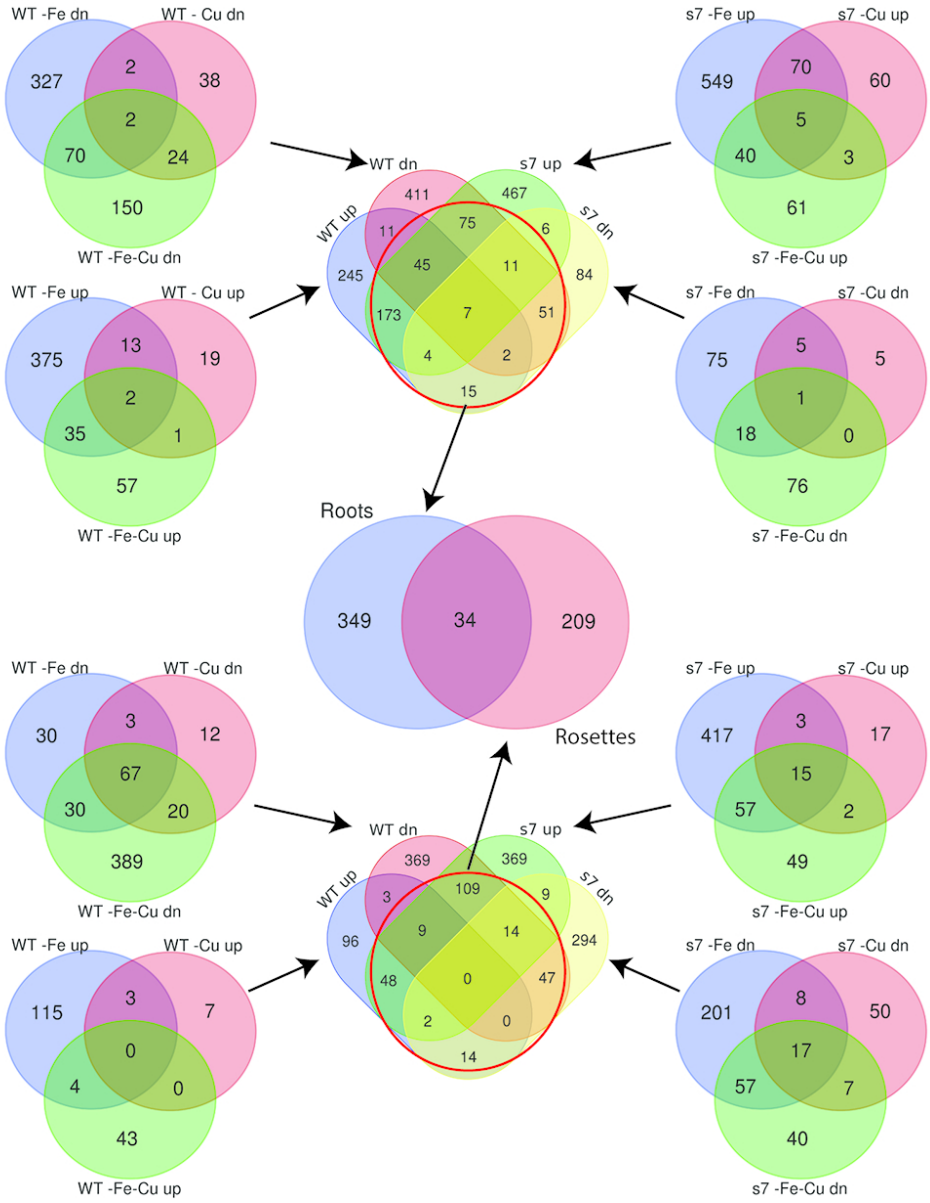

Figure 4. Venn diagram series used to isolate potential Fe-Cu crosstalk genes. Outer Venn diagrams on the upper half are genes from WT (left) and spl7 (right) that were upregulated or downregulated in -Fe, -Cu, or -Fe-Cu treatments. Outer Venn diagrams on the lower half are genes from WT (left) and spl7 (right) that were upregulated or downregulated in -Fe, -Cu, or -Fe-Cu treatments. The center upper (roots) and lower (rosettes) Venn diagrams contain all genes that were upregulated or downregulated in any of the -Fe, -Cu, or -Fe-Cu treatments in WT or spl7 mutants. The red circle shows genes that were advanced to the central Venn diagram that contains likely Fe-Cu crosstalk genes in roots and/or rosettes.

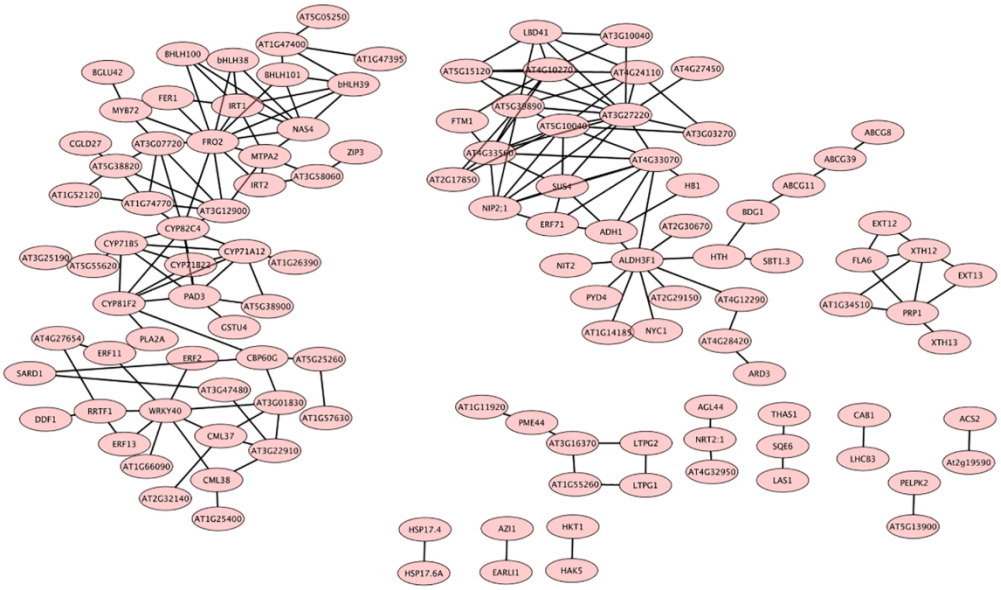

Figure 5. Gene co-expression networks in roots as determined by STRING analysis and visualized in Cytoscape. The largest module on the left was designated as the Fe-Cu crosstalk module of interest.

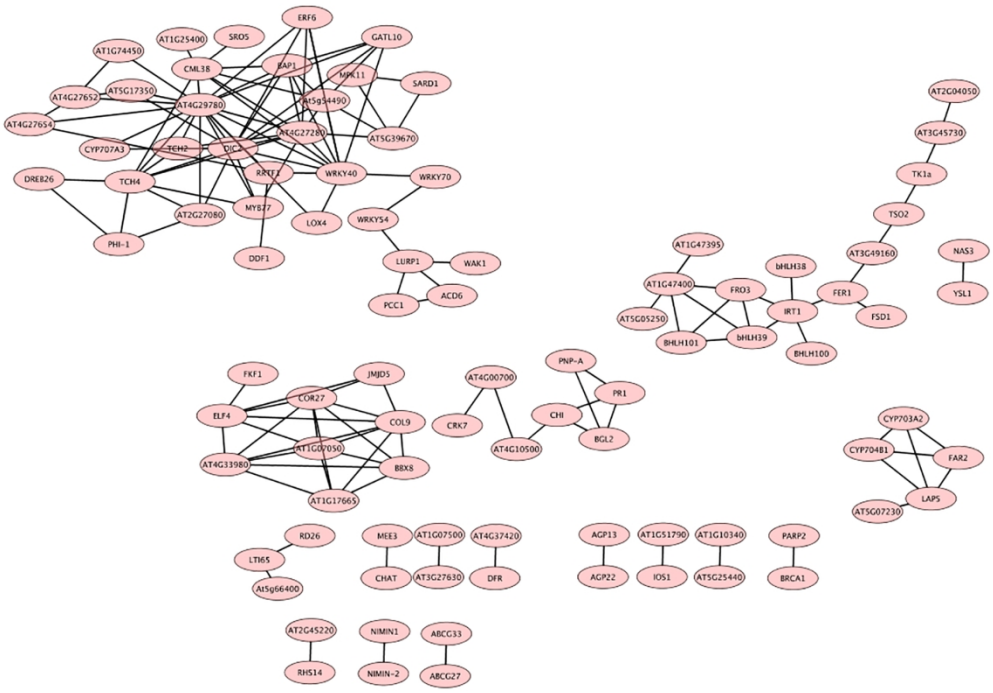

Figure 6. Gene co-expression networks in rosettes as determined by STRING analysis and visualized in Cytoscape. The second-largest module on the upper right was designated as the Fe-Cu crosstalk module of interest.

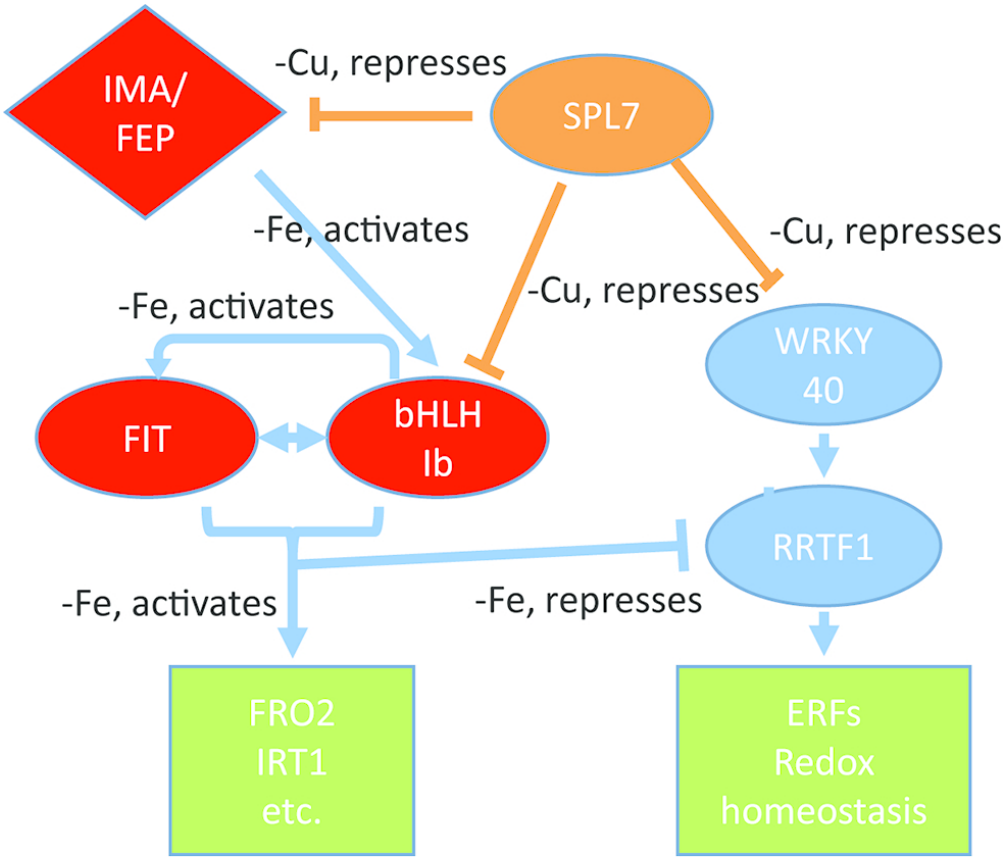

Figure 7. Model of roles of FIT and SPL7 in Fe-Cu crosstalk based on RNA-seq gene expression results. Transcription factors (FIT, bHLH Ib, SPL7, WRKY40, RRTF1) are represented as ovals; the peptides IMA/FEP are represented by a diamond, and downstream targets are represented by a green box. In this model, subgroup Ib bHLH proteins act upstream of and interact with FIT to activate Fe uptake target genes under Fe deficiency conditions. IMA/FEP peptides are upstream of subgroup Ib bHLH proteins. SPL7 protein represses (directly or indirectly) IMA/FEP and subgroup Ib bHLH expression under Cu deficiency and simultaneous Fe and Cu deficiency. SPL7 also represses WRKY40, which is upstream of RRTF1. RRTF1 is also a potential FIT target 51 and is repressed under Fe deficiency. WRKY40 and RRTF1 are upstream of the redox homeostasis network (see Table 2) which includes certain ERF proteins among others.